Measuring Individual Tree Water-use in Mature Native Species in the Pacific Northwest to Determine their Benefits for Stormwater Management

Final Report

Prepared for:

Washington State Department of Ecology

Washington Stormwater Workgroup

Prepared by:

Anand Jayakaran[1], Benjamin Leonard[1], Dylan Fischer[2], Jamie Duberstein[3], Abby Barnes[4]

[1]Washington State University

[2]Evergreen State College

[3]Clemson University

[4]Washington Dept. of Natural Resources

March 31st, 2022

Revised August 2022

Executive Summary

Managing stormwater is a serious challenge in urban areas, particularly for rapidly growing urban communities in Western Washington. Urban trees in parks, natural areas, street-side, and on private lands combined with other green stormwater control elements provide excellent opportunities to mitigate the effects of stormwater runoff in the Puget Sound. The role of trees in managing stormwater runoff in urbanizing landscapes, is an emerging area of interest.

The purpose of this project was to develop a rigorously derived hydrologic dataset that revealed how stormwater is captured by mature common native evergreen and deciduous trees based on the physio-climatic conditions of the Pacific Northwest. The tree species considered for this study included common species native to the PNW, spanning several ecosystem types for which development or redevelopment is likely to occur. General environmental data were collected to help explain tree water-use across the different study sites.

The study involved instrumenting 64 trees at two locations in the Olympia area to determine transpiration rates of four species of large native trees, comprising two evergreen and two deciduous tree species: Douglas-fir, western redcedar, bigleaf maple, and red alder. Of these, all were instrumented to measure sap flux, 36 for canopy interception, and 24 instrumented for stemflow.

Our study shows that when all the components of the hydrologic budget are summed, bigleaf maples can intercept or transpire more than the total volume of water incident on their canopies during the leaf-on season. The remaining species managed over 70% of the rainfall landing on their canopies during leaf-on. During leaf-off season, the two evergreens can transpire and intercept over half the rainfall landing on their canopies as shown below

Table E1: Leaf-on hydrologic budgets for four native tree species

	Leaf-Off		Leaf-On		Annualized Values	
Storm totals (cm)	124.8		42.9		167.6	
Median Values by Species (Transpiration + Interception)						
Tree Species	%	cm	%	cm	%	cm
Bigleaf Maple	27.6%	34.4	126.5%	54.3	52.9%	88.7
Red Alder	30.6%	38.2	76.2%	32.7	42.3%	70.9
Douglas-fir	57.2%	71.4	73.1%	31.3	61.3%	102.7
Western redcedar	63.3%	79.0	72.6%	31.1	65.7%	110.1

Native Tree Water Use
Study In Progress
Do Not Disturb

What is this study?

This study aims to quantify tree water use. Stands of native trees work as important stormwater buffers that reduce flooding and prevent toxic runoff from entering sensitive streams and rivers.

What are the trees wearing?

Underneath a layer of heat protective insulation a set of probes measure the tree's water use. This is done by measuring the temperature of two matched probes. Water movement up the tree's stem cools the probes. Over time it is possible to relate this data to the flow rate of water traveling from the tree's roots to its leaves.

Rainfall Evapotranspiration

Paired Probes

Weather Insulation Datalogger
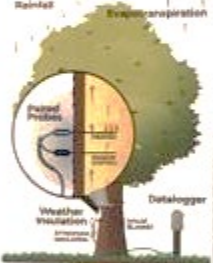
Collaboration

This study is a special collaboration between Washington State University, Clemson University, the Washington Department of Natural Resources, and the Evergreen State College, with funding provided by the Washington Department of Ecology.

For more information, please contact:
Dylan Fischer, Ph.D.
fischerd@evergreen.edu
(360) 867-6509

evergreen

1. Introduction

Trees in forested watersheds are known to manage large volumes of runoff through interception and transpiration. Trees not only intercept rainfall with their canopies (*Interception*), but also are capable of removing water from soils with their extensive root systems (*Transpiration*). In the face of urban development, surfaces that typically absorb rainfall like trees and natural soils are replaced with impervious surfaces like roads, pavements, and roofs. This alteration of the landscape for urbanization has serious hydrological consequences, where large amounts of stormwater runoff are generated causing flooding and the transport of pollutants to sensitive receiving waters. Therefore, the reintroduction of trees, and the retention of older trees to limit the damage produced by unmitigated stormwater runoff in urbanizing landscapes, is an area of much recent interest (Berland et al. 2017; Kuehler et al. 2017; Carlyle-Moses et al. 2020).

Trees in urban landscapes offset stormwater runoff by reducing the amount of stormwater that might be generated from that landscape through interceptive and transpirative processes. To maximize the stormwater benefits provided by trees it is important to understand the environmental and physiological factors affecting tree water-use, and developing tree-water use for common tree species in their native environments.

1.1. Study Need

Urban trees in parks, natural areas, street-side, and on private lands combined with other green stormwater control elements provide excellent opportunities to mitigate the effects of stormwater runoff in the Puget Sound. While the runoff mitigation potential of forest or large tree stands is well known, there is still the need to quantify stormwater mitigation values associate ed with individual trees.

The purpose of this work was to develop a rigorously derived hydrologic dataset that showed how stormwater is captured by existing common native evergreen and deciduous trees, based on the physio-climatic conditions of the Pacific Northwest. Residual forests and native trees provide stormwater mitigation as well as a host of other ecosystem services, however retention is generally the last option during development activities; trees are frequently removed and the on-site capacity to mitigate stormwater is lost. Information derived from this work offers valuable insight on the hydrologic value of existing trees. A proper valuation of individual trees and the direct measurement of transpirative processes is a central tenet of this work.

The study was based on instrumenting individual trees at the Evergreen State College campus and the Webster Nursery Farm, both sites in Olympia, WA. The trees were

instrumented with sensors that measured interception, stemflow, transpiration, and localized soil moisture. When combined, data from these sensors provided a complete view of how much rainfall was managed by an individual trees, or in simple terms, the rainfall that did NOT end up as stormwater runoff.

2. Methods

2.1. Study Design

The study involved instrumenting 64 trees at two locations in the Olympia area to determine transpiration rates of four species of large (>12" DBH) native trees, comprising two evergreen and two deciduous tree species. Of these 64 trees, all were instrumented to measure sap flux, 38 for canopy interception, and 24 instrumented for stemflow.

The two locations were The Evergreen State College and the Webster Nursery Farm. At each of the two locations, a weather station was installed to measure microclimatic variability. At each location, four plots of trees were targeted for instrumentation giving a total of 8 plots between the two sites. Amongst these 8 plots, 32 deciduous and 32 evergreen trees were identified for further instrumentation. Each of the 8 tree plots were monitored for variation in soil moisture over the period of study. The work was carried out over two years, starting in May 2019, and ending in May 2021.

2.2. Study Site

The two study locations in the south Puget Sound region near Olympia, WA were located at The Evergreen State College and Webster Forest Nursery (Evergreen and Webster; Figure 1). The sites are 8.7 miles apart from each other (Euclidean distance), or approximately 15 minutes (11.9 miles) by vehicle. Despite their proximity these locations experience slightly differing micro-climates due to unique geographical features such as the Puget Sound and the Black Hills. Sites represented locations that would typically face development in a rural-urban interface, the interface that is seeing the greatest land use changes in western Washington.

Both locations were identified as forested, but better described as managed forest stands interspersed with agricultural practices, buildings, and a parking lot. Based on historic aerial imagery and local knowledge both sites were last subject to timber harvesting in the 1950s and 60s making many of the mature trees at least 50 years old. Critically, both sites offered power, security, and full-time equipment access. While a variety of forest habitat conditions were present across sites, all plot locations were free from invasive plant species

prevalent in western Washington that may impact tree health such as English ivy, scotch-broom, and Japanese knotweed.
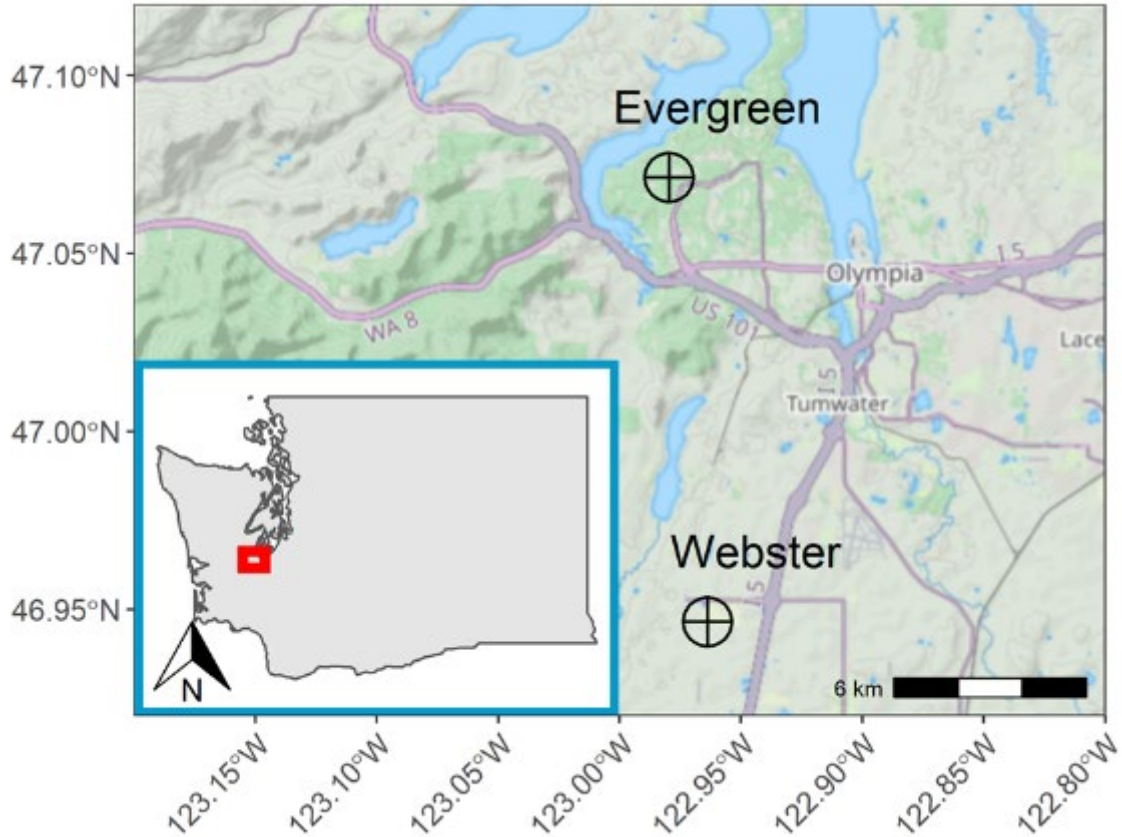
Figure 1: Map of the south Puget Sound region of Washington State showing the two study locations (Evergreen and Webster).

2.3. Tree Selection

Of the many differences between candidate tree species, it was decided that the difference between evergreen and deciduous species would have the greatest study impact from an eco-hydrological perspective. Therefore, two of each type were chosen based on over-all prominence in the region and availability at each of the study sites. Douglas-fir and western redcedar and evergreen conifers while bigleaf maple and red alder are deciduous broadleaf species. The trees chosen for this work comprised 17 Red Alder, 15 Bigleaf Maple, 21 Douglas Fir, and 11 Western Redcedar trees.

Douglas-fir were by far the most abundant tree at both sites and their presence at each study location provided a convenient comparison for assessing each deployment. Douglas-fir are also the most abundant tree in Washington state and are expanding in range due to recent shifts in forest composition and structure (Stanke et al. 2021). They are a commodity staple in the state's timber industry and are easily recognized by their spiraling needles, three-lobed cone bracts, deep-pitted bark, and overall grandeur in mature second-growth lowland forests (Figure 2; Figure 3). Typical mature height is around 125 feet; however, the tree can grow to be over 250 feet tall and 30 inches in diameter (Earle 2021; WSU 2022).

Western redcedar tends to grow in well-established lowland groves and was the least common tree between plots, only occurring at two locations. It has been called "the tree of life" and "the cornerstone of northwest coast Indian culture" having been used for canoes, baskets, clothing, shelter, medicine, and even food (MacKinnon et al. 2016). The commercial value of this tree was realized in the 20th century and most old-growth specimens have now been lost to logging. These trees are very visually distinct with large, fluted trunks, scaley leaves forming branchlets, drooping boughs, and voluminous canopies. Western redcedar, Thuja plicata, is much larger than other species in its genus and bears some likeness to California coastal redwoods (*Sequoia sempervirens*) and giant sequoias (*Sequoiadendron giganteum*).

Bigleaf maple showed the greatest variability in terms of size and appearance throughout study locations. While the bark is often obscured by dense ferns, mosses, and lichens, bigleaf maples can be identified by their large 5-lobed palm-shaped leaves during leaf-on (OSU 2022). Large drooping flower-clusters and brown fuzzy double-winged "helicopter" seeds are also unique hallmarks of the species. In the study, several bigleaf maple canopies were partially suppressed by taller Douglas-fir and western redcedar but extended laterally from the under-story to achieve co-dominance. This meant that bigleaf maple canopies often covered a larger surface area than either of the taller conifers. Due to their large reach, seasonal deposition of leaves, seeds, flowers, and epiphytes are important for enriching nearby soils with regenerative organic matter.

Larger trees with well-developed canopies and trunks were chosen for the study, however, there was some overlapping of canopies as tree proximity was an important consideration when instrumenting for sap flux (shorter cable lengths, and the need to share dataloggers between trees).

Red alder was most common in lowland areas that experienced seasonal flooding and on the periphery of Douglas-fir stands. These trees grow in tight clusters, and it was common for stems and canopies to overlap. Red alder bark is smooth, white-grey and may be covered with lichen. Red alders have shallow, but extensive root networks with microbial

communities that allow for nitrogen fixation (Perakis and Pett-Ridge 2019). This not only allows red alders to grow in nutrient poor areas, but has been found to improve forest ecosystem health, increasing the size and abundance of dominant Douglas-fir (Miller and Murray 1978). Their preferred habitat is along or near riparian banks where they act as a stabilizing force against erosion (Balian and Naiman 2005; Feau et al. 2022).

Figure 2: Leaf-off pictures taken of the four tree species chosen for this study with leaf shapes overlaid. All four of these pictures were taken within a public park a few hundred feet from each other demonstrating how common these species are in western Washington lowland environments.

Figure 3: Photos of bark textures commonly associated with the study tree species (mature individuals). **Douglas-fir** *– very thick, corky, fire-resistant bark with deep-pitted grooves forming channelized vertical fissures;* **western redcedar** *– relatively thin, smooth, scaly bark which sheds long-thin vertical spears along bulges (flutes) that often appear towards the base of the main stem;* **bigleaf maple** *– thin bark with many small ridges and deep furrows which attract mosses, lichens, and ferns creating rich epiphyte communities (see inset);* **red alder** *– very thin papery smooth bark with clearly visible lenticels and large patches of white pencil script lichen (Graphis scripta).*

Table 1: Selection of trees included in the study by plot and species where each tree was measured for sap flux.

Site	Location	Plot #	Tree Species at Study Location			
			Douglas-fir	western redcedar	bigleaf maple	red alder
			Pseudotsuga menziesii	*Thuja plicata*	*Acer macrophyllum*	*Alnus rubra*
Evergreen	Organic Farm	1	2(1)	0	0	6(5)[2]
		2	2(1)[2]	0	6(5)[2]	0
	Parking Lot	3	0	6(1*)[3]	2	0
		4	6(1*)[1]	0	1[1]	1[1]
Webster	North Field	5	2(2)[1]	0	0	6(3)[1]
		6	5(5)[1]	0	1(1)	2(1)
	South Field	7	1(1)	5(4)[3]	2(1)	0
		8	3(3)[1]	0	3(2)[3]	2(1)[2]
Total	64(38)[24]		21(14)[6]	11(5)[6]	15(9)[6]	17(10)[6]
Notes	*Parentheses, "()", indicate the number of trees with throughfall troughs and rain gauges. Asterisks, "*", are placed next to the parking lot trees which used a series of rain gauges since troughs were not feasible at the location. Brackets, "[]", indicate the number of trees with stem flow collars and buckets.*					
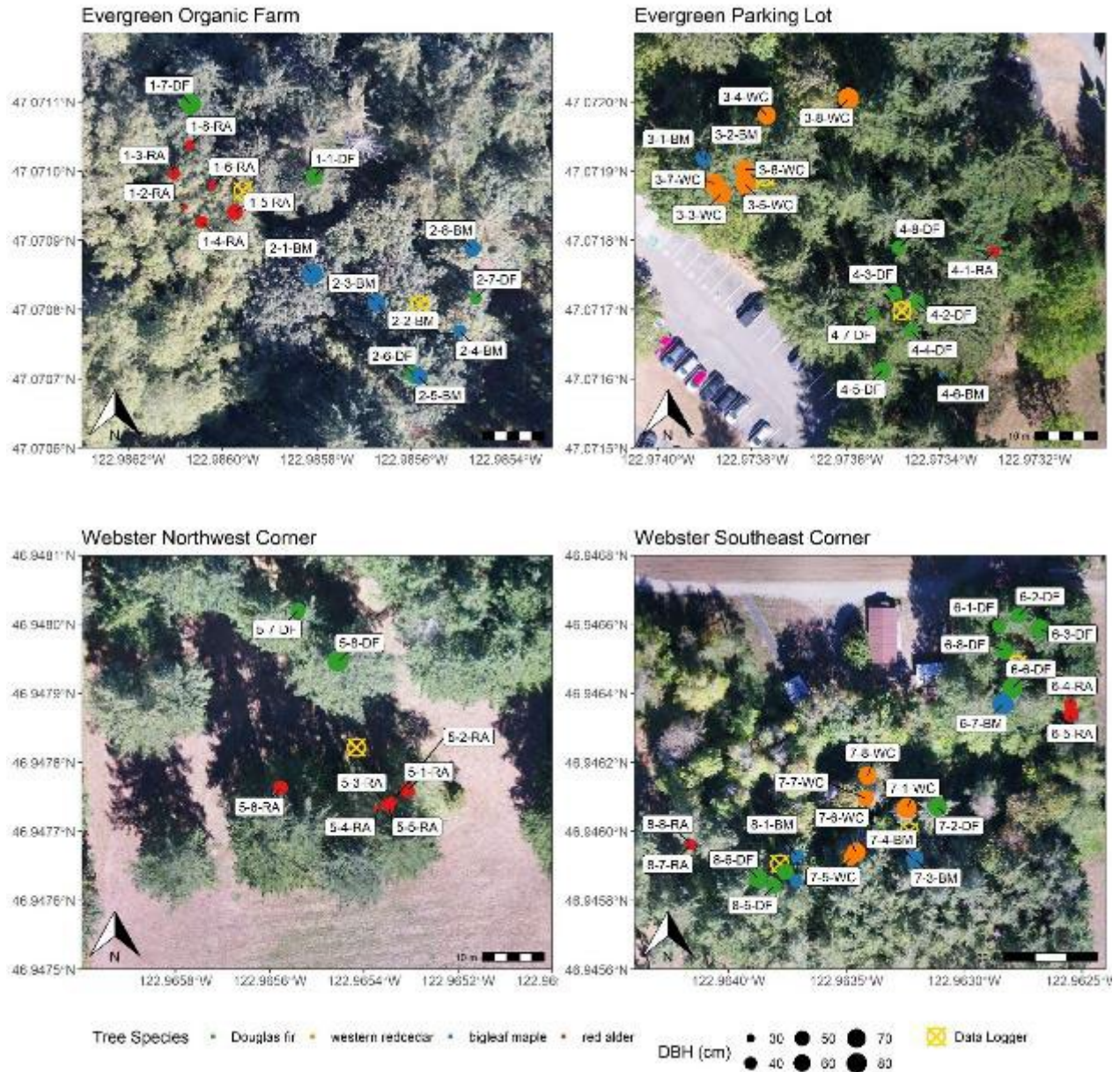
Figure 4: Individual tree locations with diameter at breast height (DBH) and data loggers plotted on top of 0.1-meter resolution orthographic imagery obtained during leaf-on conditions in early September 2021. Scale for the "Webster Southeast Corner" was increased by 2x to capture the full spatial extent of 3 plots.

11
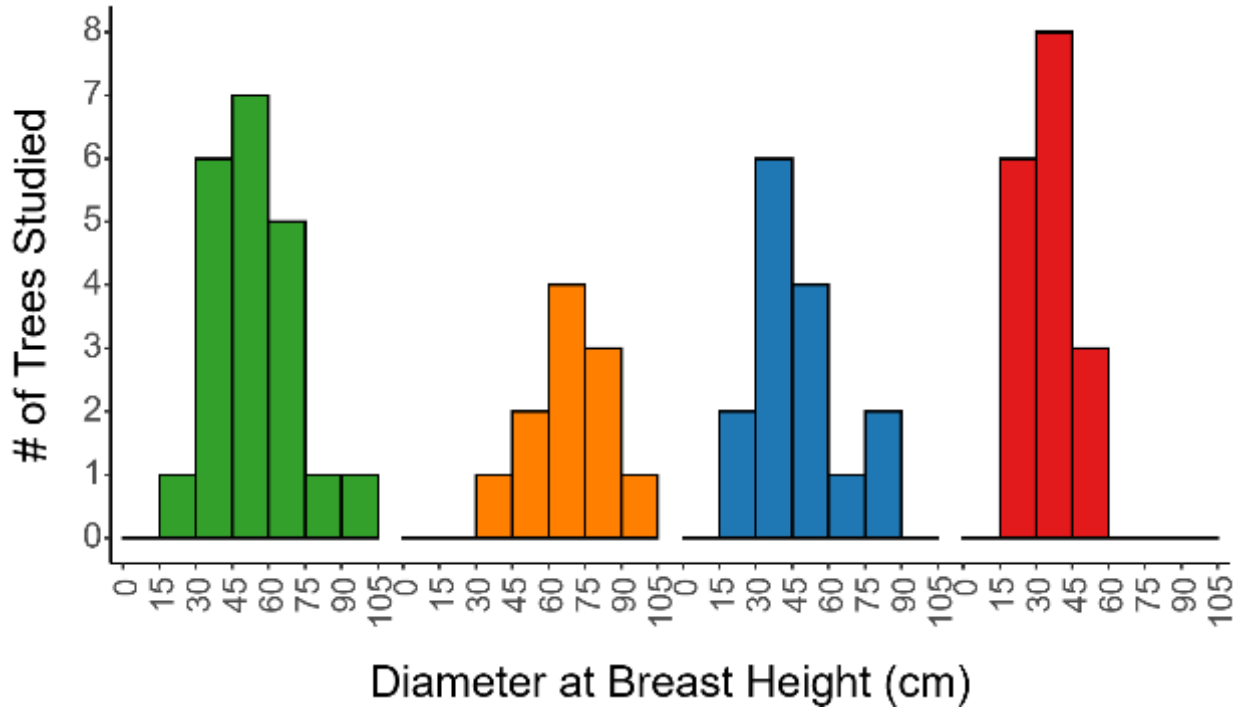
Figure 5: Histogram of tree size distributions per species using tree diameter at breast height (DBH) in 15 cm bins. Note that the most common size bin was 30 to 45 cm for bigleaf maple and red alder, 45 to 60 cm for Douglas-fir and 60 to 75 cm for western redcedar.

2.4. Measurements

2.4.1. Environmental Data

General environmental data were collected to identify general site-specific climate trends and to develop final tree water-use calculations for interception and transpiration (Table 2). Of greatest importance, precipitation data were needed to delineate storm events and calculate water-use in relation to the amount of total rainfall for a period of interest. These rain gauges were attached to larger weather stations that collected a variety of other measurements used to assess ambient conditions. Other environmental data were collected with separate equipment deployments for plot specific soil moisture and canopy temperature and relative humidity.

Some of this data was used to explain direct measurements of water-use. For example, it was expected that transpiration rates should be impacted by several variables including: a) the intensity of photosynthetically active radiation (PAR), b) the availability of soil water in the root zone (soil moisture), and c) the potential direct evaporation of water from a leaf's surface as dictated by the vapor-pressure deficit (VPD). VPD is calculated from measurements of air temperature, relative humidity, and atmospheric pressure (Appendix A – Methods: Soil Moisture Probes and Canopy VPD Sensors).

Parameters such as leaf wetness, wind speed, and soil temperature may be interpreted more qualitatively to better understand the general micro-environments each site operates within.

Table 2: Summary of all equipment deployments with number of sensors and installation dates for each site. Environmental data equipment deployments not associated with direct individual tree water-use measurements is in bold.

	Date of First Deployment		# of Sensors
	Evergreen	Webster	
Weather Station	26-Apr-19	30-Apr-19	9 per site[a]
Sap Flux Station	16-Jun-19	17-May-19	4 per site[b]
Canopy VPD	1-Aug-19	17-Jul-19	5 total[c]
Plot Soil Moisture	26-Aug-19	9-Sep-19	5 per plot[d]
Throughfall	1-Sep-19	1-Sep-19	38 total[e]
Stemflow Collars	31-Jan-20	31-Jan-20	24 total[f]

Notes: [a] 13 variables from 9 sensors; [b] 8 trees per site and 1 to 2 sensors per site; [c] 2 at Evergreen and 3 at Webster due shared canopies at plots 1+2, 3+4, and 7+8; [d] Not deployed at Evergreen parking lot until fall 2019 due to need for underground cable mapping; [e] Two sets of rain gauges at 0', 5', and 10' used for two trees at Evergreen parking lot rather than troughs; [f] 6 per species evenly divided by site.

Weather Stations and Data Loggers

Weather stations were set up in fields at the Evergreen Organic Farm and north Webster at least 300 feet from any obstructing objects (trees, buildings, etc.) and stabilized with guywires and grounding anchors (Figure 6). A total of 13 parameters were recorded by each weather station (Table 3). Additional rain gauges not associated with the established weather stations were deployed under tree canopies to measure throughfall. All weather stations, soil moisture, VPD, and rain gauge sensors recorded measurements every minute. Data were uploaded to the *Hobolink* cloud using a *RX-3000* data logger every hour. Weekly data summaries were downloaded and post-processed to average measurements every 15-minutes.

Figure 6: Weather station placed in a field north of the Webster plots. Additional nearby weather stations used by AgWeatherNet were used for data quality assurance.

Table 3: List of weather station parameters measured. Units are in parentheses.

Weather Station Parameter	Range of Values
Air Temperature (°C)	-7.6 to 37.5
Dew Point (°C)[a]	-10.5 to 24.5
Gust Speed (m/s)[b]	0 to 9.4
Leaf Wetness (%)	0 to 100
PAR (µE)	1 to 2377
Pressure (mbar)	660 to 1031.9
Rain (mm)	0 to 13.7
RH (%)	0 to 100
Soil Moisture (m^3/m^3)[c]	0 to 0.4
Soil Temperature (°C)	0.9 to 29.4
Solar Radiation (W/m2)	1 to 1204.7
Wind Direction (°)	0 to 358
Wind Speed (m/s)	0 to 5.7

Notes: [a] Calculated from air temperature and relative humidity (RH); [b] Calculated from wind speed; [c] Upper limit was chosen based on the upper limit for reliable measurements using capacitance soil moisture probes.

Soil Moisture Probes and Canopy VPD Sensors

Additional plot-level soil moisture probes and hanging canopy temperature/relative humidity sensors, to measure VPD, were deployed as appropriate (Table 2). Respectively, the purpose of this data collection was to:

> a) Provide a general assessment of soil moisture variability between plots and weather stations with an emphasis on identifying drought and flood conditions at the root level (12 to 18 inches below ground depending on where most of the root mass was present).

> b) Provide a robust assessment of atmospheric conditions near where gases are exchanged during transpiration at the canopy level (50 to 100 feet above the ground depending on where most of the foliage was present).

Details related to these deployments is available in Appendix A – Methods: Soil Moisture Probes and Canopy VPD Sensors.

2.4.2.   Interception Estimates

Throughfall

A total of 38 trees were instrumented for the measurement of canopy throughfall; 36 with troughs made from cut PVC pipes directed into rain gauges and 2 with rain gauges alone (Table 1). In either case, throughfall was determined in-situ by comparing closed-canopy measurements to open-canopy weather stations using the respective collection surface area ratios and several other correction factors to normalize values (See Appendix-Methods for more information)

For trough systems, two randomly placed radial troughs extended 10 feet from the tree bole to near the tree canopy drip line (Figure 7). This configuration was approximated by individual rain gauges at the parking lot where t-posts could not be used to secure troughs. Details on the setup of these systems and calibration steps performed are in Appendix A – Methods: Throughfall. Throughfall can be expressed as a depth (cm), or as a fraction of the rainfall measured in open canopy.

$$Throughfall_i(cm) = \sum Precipitation_{cc_i} * Factor_{a,b,c} \qquad (1)$$

$$Throughfall_i(\%) = \frac{\sum Precipitation_{cc_i} * Factor_{a,b,c}}{\sum Precipitation_{oc_i}} * 100 \qquad (2)$$

Where:

- *i* is the qualifying storm event under consideration,
- *Precipitation$_{cci}$* is the total rainfall (cm) measured during that event under the tree canopy or closed canopy (cc),
- *Precipitation$_{oci}$* is the total rainfall (cm) measured during that event under open canopy (oc),
- *Factor$_{abc}$* are correction factors that account for the dimensions of the openings in the rain gages and interception troughs that include:
    a) the difference in collection surface areas between individual troughs,
    b) rain gauge specific calibrations, and
    c) a reference open-canopy system next to the weather station rain gauge at Webster.

For more details on throughfall methods used, please see the Appendix A

Figure 7: Arrangement of throughfall troughs.

Stem Flow

Stemflow was collected by affixing collars designed to channel water to collection buckets around the bole of 24 trees (Table 1; Figure 8). Collected stemflow volumes were then measured volumetrically with a graduated cylinder, or by weight with a scale if the volume exceeded several liters. Stemflow was monitored regularly and collected after large storm events or every other week during winter months. Collected volumes were compared to the tree's canopy area to calculate stemflow as a percent of total canopy rainfall (Equation 3).

Since reporting stemflow in terms of canopy area was most useful for tree water budget calculations this value was used in most analyses. See Appendix A – Methods: Stem Flow for more detail.

We calculated stemflow using the following equations:

$$Stemflow_{i,j,k}(cm) = \left(\frac{Collection\ Volume_i}{Canopy\ Area}\right) \quad\quad\quad (3)$$

$$Stemflow_{i,j,k}(\%) = \frac{\left(\frac{Collection\ Volume_i}{Canopy\ Area}\right)}{\sum Precipitation_{oc_{i,j,k}}} * 100 \quad\quad\quad (4)$$

Where:

- *ijk* are one or several storm events that define a collection period,
- *Collection Volume$_i$* is the volume of stemflow (cm^3) collected during a collection period,
- *Canopy Area* is the canopy area (cm^2) of the tree where stemflow was collected,
- *Precipitation$_{ocijk}$* is the cumulative rainfall (cm) that occurred over the collection period measured under open canopy (oc).

Figure 8: Stem flow buckets placed beneath stem flow collars on a Douglas-fir (left) and bigleaf maple (right) at the Evergreen Organic Farm (plot 2).

17

Interception Calculation

For every measured qualifying storm, interception was calculated by subtracting the sum of throughfall and stem flow from the total rainfall measured under open canopy – all in units of depth (cm). Interception was also expressed as a percentage of total rainfall measured under open canopy for that event.

$$Interception_i(cm) = \sum Precipitation_{oc_i} - (Throughfall_i + Stemflow_i) \quad (5)$$

$$Interception_i(\%) = \frac{\sum Precipitation_{oc_i} - (Throughfall + Stemflow)}{\sum Precipitation_{oc_i}} * 100 \quad\quad (6)$$

Where:

- $\sum Precipitation_{oci}$ *is the total rainfall (cm) associated with the qualifying storm event measured under open canopy,*
- *Throughfall$_i$ & Stemflow$_i$ (both in cm) are calculated from equations 1 & 3.*

2.4.3.   Transpiration by Sap Flux

Transpiration, a critical component of individual tree water-use, is typically calculated using direct measurements of sap flux. The thermal dissipation probe (TDP) technique for sap flux involves measuring the temperature difference between heated top and unheated bottom probes inserted into the tree's xylem. As sap moves upwards during transpiration, the heated probe is cooled and the temperature difference between probes is diminished (Figure 9).

Using the Granier equation (see Appendix A – Methods: Transpiration by Sap flux), sap flux is calculated from the TDP probe data as the flux of water per unit area of sapwood with units: cm^3 of H$_2$0/ cm^2 of sapwood/ second. The movement of sap in trees is only seen between storm events and not during a storm event simply because the vapor pressure deficit is too low during those times. Therefore, our sap flux measurements correspond only to time periods between storm events.

Sap flux is transformed to transpiration, and expressed as percentage of the total volume of rainfall falling on the canopy over the time-period being considered (whole year, season, month, etc.) using the following equation:

$$Transpiration_j(cm^3) = \sum(Sap\ Flux_b * Sapwood\ Area_b) \quad\quad (7)$$

$$Transpiration_j(\%) = \frac{\sum(Sap\ Flux_b * Sapwood\ Area_b)}{\sum Rainfall_{oc_j} * Canopy\ Area} * 100 \qquad (8)$$

Where:

- j is the time period being considered (hrs),
- b is the xylem depth where the TDP probe is inserted (cm),
- $Sap\ Flux_b$ is 15-minute sap flux measurements ($cm^3_{water}cm^{-2}_{sapwood}hr^{-1}$) at depth b,
- $Sapwood\ Area_b$ is the sapwood area (cm^2) at depth b.

We had to account for attenuation of sap flux at various depths.
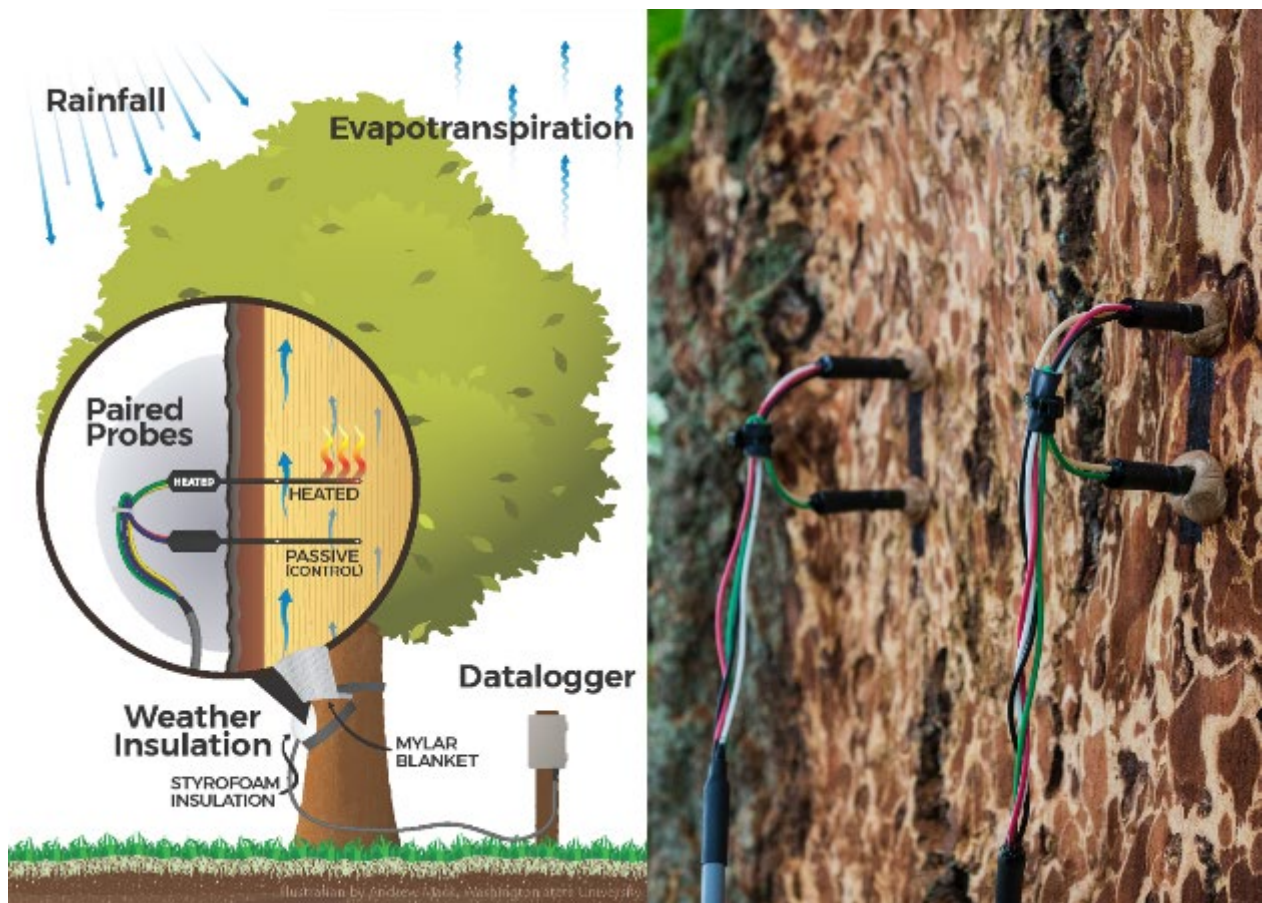
Figure 9: Diagram illustrating the thermal dissipation probe (TDP) method for measuring sap flux (left) in addition to two sets of probes inserted into a Douglas-fir (TDP-50 [left]; TDP-100 [right]) where excess bark has been removed and insulation has yet to be installed.

2.4.4.   Canopy Area by Drone Surveys

Aerial determination of canopy cover was used for calculating the surface area footprint associated with each individual tree. Considering that tree removal and replacement with impermeable surface area would result in corresponding volume of stormwater runoff generated for each rain event these values were used to express tree water-use as a percentage of total rainfall. Using this approach, accurate canopy areas proved essential in combining interception and transpiration measurements into a single framework to consider individual tree water-use in relation to their stormwater benefit.

Due to the wide variety of tree canopies studied, canopy area proved difficult to measure with traditional ground surveying equipment (densitometer, measuring tape, etc.). In 2019 and 2020, two pilot surveys were conducted at Webster Forest Nursery to assess whether photogrammetric canopy models created from UAV (drone) obtained aerial imagery could be used. These flights proved successful, offering high-resolution imagery that could distinguish individual tree canopies. Definitive imagery was obtained in March, May, and September of 2021 at both Evergreen and Webster thanks to DNR's Aquatics Program.

Structure from motion (SfM) algorithms were used to generate dense point clouds from spatially aligned images. Point clouds were then processed to create a) 2D geo-referenced orthographic images, and b) 3D canopy height models. Canopy areas were determined both a) manually from polygons traced from orthomosaics, and b) automatically from canopy height models.

2.5. Individual Tree Water Budgets

2.5.1. Leaf-On/Off Determination

Calendar months were divided into leaf-on and leaf-off categories based on the leaf phenology of the deciduous species (bigleaf maple and red alder) which underlies general weather patterns of the pacific northwest. While imprecise, this allowed for a seasonal comparison between tree species and separated out months with the greatest stormwater potential (leaf-off).

Leaf-out in bigleaf maple and red alder typically occurs in late April and early May following their initial reproductive cycle. Reproductive bud-burst results in catkins (flowers) which have been observed on red alders at Webster around the second week of March (Prevéy and Harrington 2018). Bigleaf maple flowers open slightly later in March and April (Budburst 2022; USFS 2022). Male (staminate) catkins usually form a few days before female (pistillate) catkins. Coinciding or succeeding with germination, the first leaf-buds may be observed in these species starting early April. Leaf-out is not complete (leaf-on) until the majority of leaves have unfolded and are actively photosynthesizing which usually does not occur until May. For simplicity, for this study we have chosen the months of May to October as "leaf-on" and November to April as "leaf-off".

Table 4: Months designated as leaf-on and leaf-off

Season	Calendar months
Leaf-on	May to October
Leaf-off	November to April

2.5.2. Qualifying Storm Events

Rainfall data from weather stations was segmented into discrete storm events for each site using predefined criteria. Qualifying storms were determined with inter-event time definitions (IETD) (Restrepo-Posada and Eagleson, 1982; Adams and Papa, 2001) based on Ecology's qualifying stormwater event criteria for stormwater discharge monitoring (Ecology 2016)[1]. In short, a rolling window was applied to 15-minute cumulative precipitation time series data for each site. Within this window, individual storms were identified based on criteria described in Appendix A - Methods

---

[1] Analyzed with R v4.1.1 (R Core Team 2021) & IETD package v1.0.0 (Duque 2020).

2.5.3.   Total Tree Water Budget Calculations

The total tree water budget can be thought of as the fraction of rainfall that is assimilated by a tree through transpiration and interception. It can be expressed volumetrically (cm³), or as a fraction (%) of the total rainfall falling on that tree's canopy area (cm²) over a specific period of time. Expressed volumetrically, the tree water budget is:

$$Tree\ Water\ Budget\ (cm^3) = Transpiration(cm^3) + Interception(cm^3) \qquad (10)$$

This assimilated water or the tree's water budget, is stormwater volume that is avoided or removed from runoff conveyance systems. In volumetric terms this runoff volume (cm³) is:

$$Runoff(cm^3) = [Precipitation * CanopyArea] - TreeWaterBudget \qquad (11)$$

We define Interception (cm³) as:

$$Interception\ (cm^3) = [Precipitation * CanopyArea] - (Throughfall + Stemflow) \quad (12)$$

Substituting *Interception* (Equation 12) into Equation 10, a comprehensive measure of a tree's water budget can be calculated as follows:

$$Tree\ Water\ Budget_n(cm^3) = \sum_{i=1}^{n} Transpiration_i + [Precipitation_i * CanopyArea] -$$
$$[Throughfall_i + Stem\ flow_i] \qquad (13)$$

Where:

- o   *n* is the total number of qualifying storm events over a specific time period (season, year, etc.)
- o   *i* is a particular qualifying storm.

To express the *Tree Water Budget* as a fraction of rainfall, the volumetric water budget (cm^3) was first normalized by canopy area (cm^2) using:

$$CanopyNormalizedTreeWaterBudget_i\ (cm) = \frac{Tree\ Water\ Budget_i}{Canopy\ Area} \qquad (14)$$

Then the *Tree Water Budget* expressed as a fraction of the total precipitation (qualifying storm totals, units = cm) that occurred over the year was calculated by:

$$TreeWaterBudget_{year}(\%) = \frac{\sum_{i=1}^{n} CanopyNormalizedTreeWaterBudget_i}{Annual\ Qualifying\ Storm\ Total} * 100 \qquad (15)$$

Where:

- n is the total number of qualifying storm events over the whole year
- i is a particular qualifying storm.
- *TreeWaterBudget$_i$* is the tree water budget per qualifying storm (cm^3)
- *Annual Qualifying Storm Total* is the cumulative qualifying storm precipitation total (cm) over the year

Similarly, the *Tree Water Budget* for the leaf-on season was calculated by:

$$TreeWaterBudget_{leafon}(\%) = \frac{\sum_{i=1}^{n} CanopyNormalizedTreeWaterBudget_i}{Leaf\ on\ Qualifying\ Storm\ Totals} * 100 \qquad (16)$$

Where:

- n is the total number of qualifying storm events that occurred over the two leaf-on seasons
- i is a particular qualifying storm during the leaf-on season.
- *TreeWaterBudget$_i$* is the tree water budget per qualifying storm (cm^3)
- *Leaf-on Qualifying Storm Total* is the sum of all qualifying storm precipitation totals (cm) that occurred over the two leaf-on seasons.

3.Results & Discussion

3.1. Qualifying Storm Events

Over the two years of this study, a total of 91 qualifying storm events were measured at Evergreen, and 93 at Webster. Of these 184 qualifying storms, 116 were events that occurred during leaf-off, and 68 occurred during leaf-on. There were 190 storm events that were non-qualifying and summary statistics are shown in Table 5 across all 374 storms. It should be noted that many qualifying storm events occurred simultaneously at both sites, but with slightly different starting and ending times. For these analyses, storm events were separated by site. A summary of qualifying storm events is presented in Table 5.

Table 5: Summary of storm characteristics for qualifying throughfall events over two years of data collection. Summary of all events including non-qualifying storms in the last column.

	Qualifying storm statistics		Overall storm statistics (Qualifying and non-qualifying events)
	Season: Leaf-On	Season: Leaf-Off	2 year summary across seasons
Number of storms	68	116	374
Min of Duration (hr)	2	3.5	0.25
Max of Duration (hr)	50.5	54.5	106
Mean of Duration (hr)	14.0	19.1	15.5
Min Rainfall Depth (mm)	5.2	5.0	0.6
Max Rainfall Depth (mm)	74.4	77.8	186.6
Mean Rainfall Depth (mm)	17.3	19.7	17.7
Min Intensity (mm/hr)	0.4	0.2	0.2
Max Intensity (mm/hr)	3.6	3.4	19.7
Mean Intensity (mm/hr)	1.3	1.1	1.3

3.2. Stemflow Estimates

Stemflow, normalized by precipitation and canopy area, was measured for 24 trees across 146 to 166 qualifying rainfall events. All stemflow data were normalized by the canopy area for that tree. Our results show that stemflow as a fraction of precipitation falling on the canopy of a tree was small, less than 1.0 % of total precipitation. Stemflow was greater during leaf-off than the leaf-on season for every species. Given there is little to no canopy to intercept precipitation during leaf-off, observing higher stem flow is expected.

The highest stemflow recorded was 0.82% of total storm precipitation during one storm event for a red alder. Of the four species measured, red alder trees showed the greatest stemflow values overall, while western redcedar had the lowest. We hypothesize that the smooth bark of the red alder trees facilitated the channeling of stem flow from the tree canopy to the point of measurement at the tree trunk, hence the high stemflow observations.

Even though all the trees in the study experienced the same distribution of storm events, how rainfall manifested as stemflow varied by species. The majority of stemflow data were left-skewed. This is true of all Douglas-fir and western redcedar collections and mostly true of bigleaf maple collections except one small, smooth-barked bigleaf maple tree. Red alder data, except for one that was suppressed by a large Douglas-fir, were more widely distributed. The number of low-volume collections dominated the distribution of stemflow data and imply low stemflow volumes are typical. However, the wide distribution of stemflow data implies that a tree can produce a wide range of stemflow volumes driven by the presence or absence of canopy, or the intensity and duration of the storm event.

Table 6: Seasonal and annualized stemflow calculations

	Leaf-Off		Leaf-On		Annualized Values	
Qualifying storm totals (cm)	57.1		24.3		81.4	
Median Stemflow by Species						
Tree Species	%	cm	%	cm	cm	%
Bigleaf Maple	0.032%	0.02	0.003%	0.00	0.02	0.023%
Red Alder	0.213%	0.12	0.092%	0.02	0.14	0.177%
Douglas-fir	0.085%	0.05	0.008%	0.00	0.05	0.062%
Western redcedar	0.054%	0.03	0.002%	0.00	0.03	0.038%
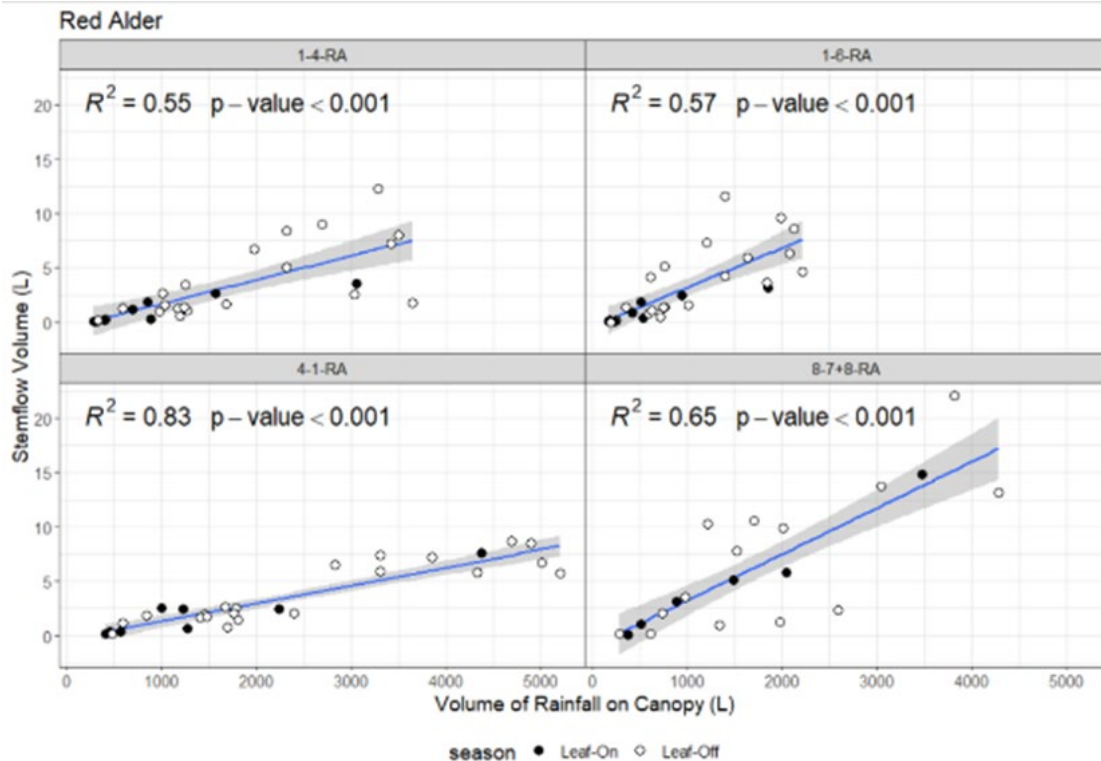
Figure 10: Volume of rainfall on canopy vs. stemflow volume for red alder collections.

Red alder trees produced the most stemflow, and stemflow observations were evenly distributed across a range of total precipitation. The other three species showed stemflow data distributions that were markedly biased towards low fractions of storm precipitation. Therefore, from least to highest, the order of stemflow generation by species is western redcedar, bigleaf maple, Douglas-fir, and red alder (Table 6).

Linear relationships between canopy rainfall and stemflow volume were observed for red alder (Figure 11), suggesting there are well-connected routes for water to move from the tree canopy to the tree trunk of red alder trees. This linear relationship was not observed for the other tree species suggesting that more rainfall on those canopies did not automatically translate into greater stemflow. We believe there are other considerations affect the generation of stemflow – like interruptions to the flow path of water by mosses, rough bark that absorb or shed water.

3.3. Throughfall and Interception Estimates

Usable throughfall data was measured at 36 trees. Two Douglas-fir were dropped because of damage to a throughfall trough, and one canopy was discovered to be suppressed by surrounding tree canopies. Results are bifurcated by season with all species represented by leaf-on and leaf-off estimates.

Throughfall estimates revealed that western redcedar trees were associated with the lowest throughfall totals, and red alders experienced the most throughfall. Of the two deciduous species, bigleaf maple showed the greatest change in throughfall between leaf-off and leaf-on conditions. Throughfall estimates are further summarized in Table 6.

Table 5: Seasonal and annualized throughfall calculations

	Leaf-Off		Leaf-On		Annualized Values	
Qualifying storm totals (cm)	57.1		24.3		81.4	
	Median Throughfall by Species					
Tree Species	%	cm	%	cm	%	cm
Bigleaf Maple	72.4%	41.3	39.3%	9.6	62.5%	50.9
Red Alder	69.1%	39.5	60.7%	14.7	66.6%	54.2
Douglas-fir	44.5%	25.4	36.7%	8.9	42.2%	34.4
Western redcedar	37.7%	21.5	36.0%	8.8	37.2%	30.3

Interception rates were calculated by subtracting the sum of throughfall and stemflow values from the total open canopy precipitation - equation 5 for *Interception* as a depth (cm), and equation 6 for *Interception* as a fraction (%).

Our interception results show that on an annual basis, western redcedar intercept the most precipitation (62.8%), and red alder the least (33.2%). It should be noted that the percentages shown here are based on qualifying storm totals, and not the total annual precipitation. Interception estimates are further summarized in Table 7.

Table 6: Seasonal and annualized interception estimates

	Leaf-Off		Leaf-On		Annualized Values	
Qualifying storm totals (cm)	57.1		24.3		81.4	
	Median Interception by Species					
Tree Species	%	cm	%	cm	%	cm
Bigleaf Maple	27.6%	15.8	60.7%	14.8	37.5%	30.5
Red Alder	30.6%	17.5	39.2%	9.5	33.2%	27.0
Douglas-fir	55.4%	31.6	63.3%	15.4	57.7%	47.0
Western redcedar	62.3%	35.5	64.0%	15.6	62.8%	51.1

During the leaf-on season and based on median values, evergreen trees intercepted more rainfall that deciduous trees. Of the two evergreen species, western redcedar intercepted slightly more rainfall (64.0%) than Douglas-firs (63.3%) during leaf-on. And for the same leaf-on season, bigleaf maples intercepted a greater fraction of precipitation (60.7%) compared to the other deciduous tree species - red alder. We also observed that the deciduous trees intercepted some rainfall during leaf-off. Overall, evergreen trees intercepted more rainfall per unit canopy area than deciduous species during leaf-on and leaf-off seasons.

3.4.   Transpiration Estimates

Due to some data loss and noise in the observed sap flux data streams, data from eleven trees with the most complete sap flux datasets were used. As with previous components of the tree water budget, all sap flux data were reduced to fractions of the total rainfall measured during the leaf-on or leaf-off seasons. It is important to note that transpiration occurs between storm events and, therefore, transpiration represents a tree's hydrologic functioning when it is not raining. Therefore, our transpiration data were aggregated on a monthly basis, and then monthly median values were calculated with the two-year dataset.

Measurements of sap flux densities across the four species showed that VPD and soil moisture were influential parameters in determining sap flux in the trees (Figure 12). During the leaf-off season (November to April), transpiration is limited by low VPD (Figure 11-row 1). Conversely, when VPD starts increasing in April, evergreen species temporarily have an advantage before the deciduous species are fully leafed-out (Figure 12-row 2). All trees were transpiring at their highest potential from May to July, thanks to optimal VPD, PAR, and soil moisture (Figure 12 -row 3). However, evergreens were not transpiring as much in August and September despite high VPD conditions (Figure 12-row 4). We hypothesize this was due to limited soil water availability resulting in drought stress. Drought stress has been found to decrease Douglas-fir growth rate (Restaino et al. 2016) and has been implicated as the main driver of a western redcedar dieback in British Columbia (Seebacher 2007; Klinka et al. 2009). In October, as the rains begin, soils become saturated again and VPD levels start to drop, all the trees begin to resemble sap flux densities similar to the leaf-off season (Figure 12 -row 5).

Expectedly, all species' transpiration was strongly correlated with vapor pressure deficit (VPD) during the leaf-on season. However, the correlation between transpiration rates and VPD was non-existent during the leaf-off season.

28
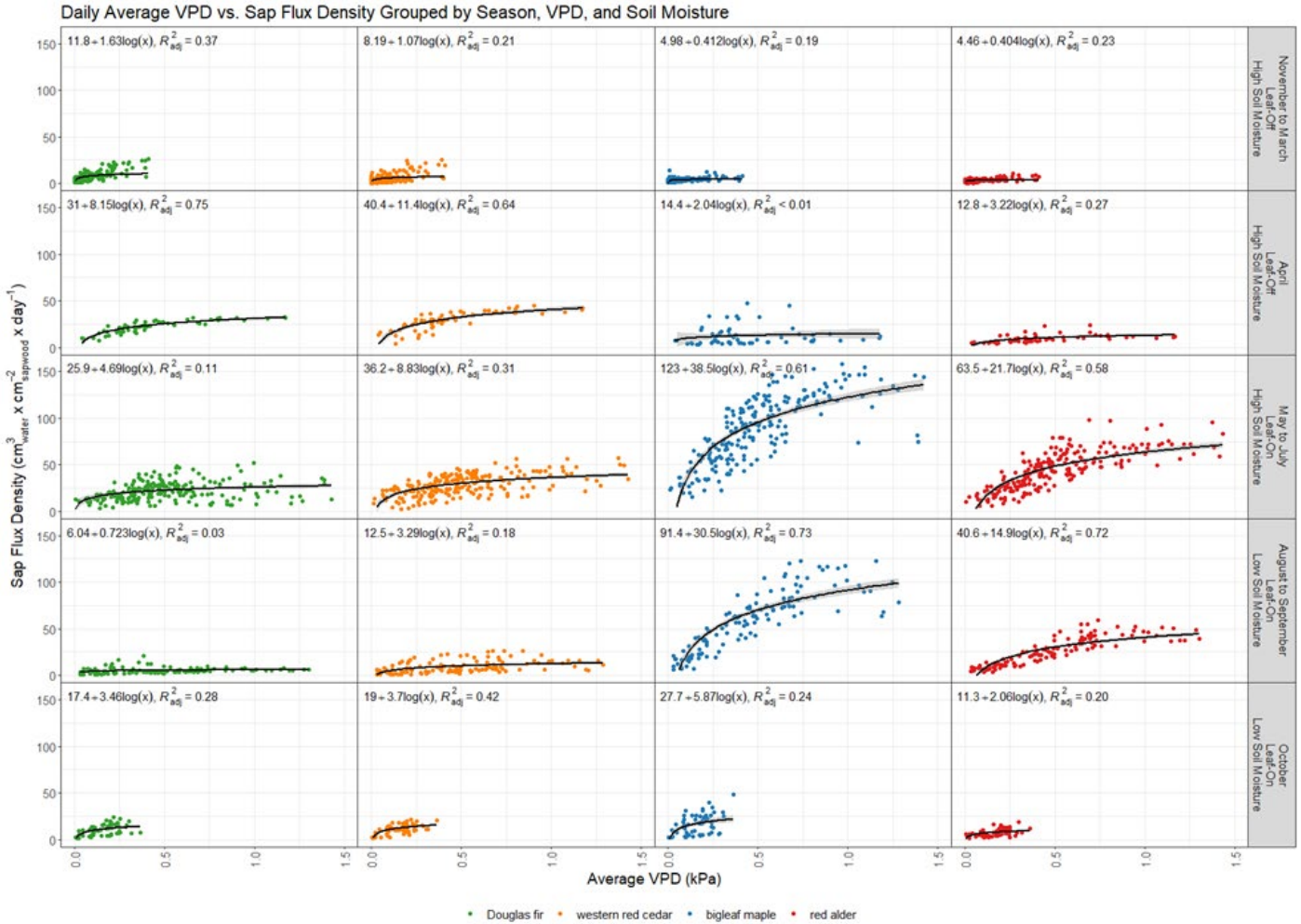
Figure 12: Daily average VPD vs. sap flux density.

Our results showed that bigleaf maples transpired the most water per unit canopy area of all the tree species measured during the leaf-on season. Bigleaf maples transpired on average 65.8% of the total rainfall measured during that season. Peak transpiration occurred in the month of July for bigleaf maples, when median transpiration was 400.6% for one of the largest bigleaf maples in the study, a volume of water that exceeds what fell directly on the tree canopy as rainfall by four times. These results suggest that bigleaf maples draw water from deeper strata in the soil profile or regions beyond the tree's dripline. Similarly, the other deciduous tree, red alder, had median leaf-on transpiration rates of almost 36.9%. Red alder also experienced peak transpiration rates in the month of July, when median transpiration rates were 223.6%. Both species of trees showed transpiration rates above 100% in the month of August as well. A table showing median monthly transpiration rates is presented in the Appendix B- Results.

Our results showing over 100% transpiration for the two deciduous species in July and August suggesting the need to quantify the structure and extent of the tree root system for these trees to fully appreciate their ability to "dewater" the soil profile between rainfall events.

Transpiration rates for evergreen trees during leaf-on were more modest than deciduous trees, with Douglas-firs transpiring a median of 9.8% of total rainfall in terms of a seasonal median. On a monthly basis, median transpiration for Douglas-firs was as high as 44.6% in July, and as low as 0.2% in December and January. Western redcedars transpired slightly less than the Douglas-firs (8.6%) during the leaf-on season. On a monthly basis, median transpiration for western redcedar ranged from 0.1% in December and January to 49.4% in July.

During the leaf-off season, evergreen transpiration rates were low, with medians of 2.1% and 1.0% for Douglas-fir and western redcedar, respectively. It should be noted that even though deciduous trees transpire primarily in the leaf-on season, evergreens continue that work in the leaf-off season, albeit at low rates. Also, sap flux per unit area of sapwood (or sap flux density) for evergreens outpace deciduous trees during the shoulder seasons just before the deciduous trees have started to ramp up in the spring or ramp down in the fall (Figure 18).

We did run our TDP sensors with the deciduous trees through the leaf-off period, the data were very noisy and were omitted from this report. However, those omitted leaf-off deciduous transpiration rates were likely to be lower than the evergreen values for the same time – less than 1%. A summary of transpiration rates by season and on an annual basis, are presented in Table 8.

*Table 7: Summary table of seasonal transpiration as a percentage of the total precipitation for leaf-on conditions. * Deciduous leaf-off data were shown as zeros due to noisy data.*

	Leaf-Off		Leaf-On		Annualized Values	
Annual average storm totals (cm)	124.8		42.9		167.6	
Median Transpiration by Species						
Tree Species	%	cm	%	cm	%	cm
Bigleaf Maple	0.0%*	0.0*	65.8%	28.2	17.7%	29.7
Red Alder	0.0%*	0.0*	36.9%	15.8	10.2%	17.1
Douglas-fir	1.8%	2.3	9.8%	4.2	3.9%	6.5
Western redcedar	1.1%	1.3	8.6%	3.7	3.0%	5.0

Evergreen trees can harness the high VPD days in the early spring and late fall to continue transpiring at high sap flux density rates. In the fall, this was observed as rainfall in September and October replenished soil water content which had previously limited

evergreen transpiration. During this time, deciduous transpiration dropped rapidly at the onset of senescence prior to full defoliation (leaf-off). In late-winter/early-spring, an extended shoulder season advantage for evergreen trees was noted in March during high VPD days preceding the leaf-on transition period for deciduous trees in April.
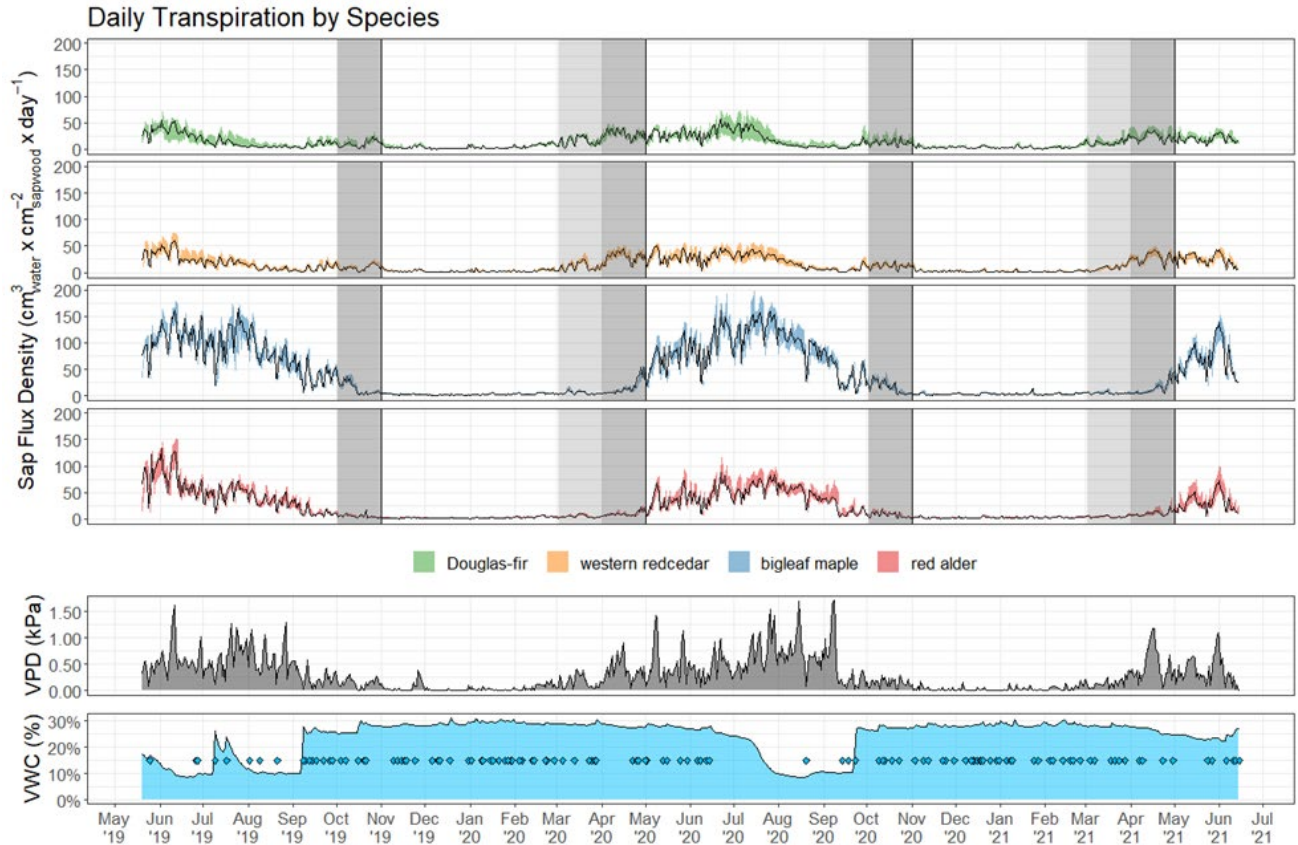
Figure 13: Temporal distributions of median daily sap flux densities by tree species with inter-quartile range (IQR) shaded. Evergreen species exhibit high sap flux densities during the shoulder season when the deciduous trees are ramping up or ramping down (dark gray). March is shaded as an extended shoulder month (light gray). Leaf-on and leaf-off are separated by a black vertical line. Plots below show average daily vapor pressure deficit (VPD) and weather station soil volumetric water content (VWC; blue diamonds indicate qualify storm precipitation).

3.5. Individual Tree Water Budgets

Our study shows that when all the components of the hydrologic budget are summed, big leaf maples can intercept and transpire more than the total volume of water incident on their canopies (126.5%) during the leaf-on season (Table 9). The remaining species managed over 2/3rd the rainfall landing on their canopies during leaf-on. During leaf-off season, the two evergreens transpired and intercepted over half of the total volume of

precipitation landing on their canopies (Table 9). During leaf-off we saw some interception by the two deciduous tree species, and small but unreported transpiration rates. On an annualized basis, the lowest contribution to stormwater removal was offered by red alder trees (42.3%), while the evergreen species prevented over 60% of the rainfall incident on their canopies from conversion to runoff. Of the four species studied, western redcedar offered the greatest contribution to runoff mitigation (65.7%), of all the tree species studied, on an annualized basis.

Table 8: Tree water budget including interception and transpiration by season and annualized

	Leaf-Off		Leaf-On		Annualized Values	
Storm totals (cm)	124.8		42.9		167.6	
	Median Values by Species (Transpiration + Interception)					
Tree Species	%	cm	%	cm	%	cm
Bigleaf Maple	27.6%	34.4	126.5%	54.3	52.9%	88.7
Red Alder	30.6%	38.2	76.2%	32.7	42.3%	70.9
Douglas-fir	57.2%	71.4	73.1%	31.3	61.3%	102.7
Western redcedar	63.3%	79.0	72.6%	31.1	65.7%	110.1

4. Conclusions & Key Findings

The study aimed to evaluate the water budget of four species of trees native to the Pacific Northwest region of the United States. The four evergreen and deciduous species are common in the region and hypothesized to play an important role in stormwater management. The water budgets of four native tree species comprising sixty-four trees were characterized by instrumenting all of them to measure transpiration, a subset of 24 for canopy interception and another subset of 12 for stemflow. The trees were spread over two sites located around the city of Olympia, WA. Weather and soil moisture at the two locations were also measured over two years.

Stemflow: Our results show that stemflow is a very small fraction of a tree's water budget. Red alder trees with the smoothest barks had the highest recorded stemflow measurements. Generally, stemflow was less than 1% of the total precipitation incident on the tree canopy. Expectedly, stemflow during the leaf-off season was higher but still insignificant.

Interception: Interception was quantified for both evergreen species during leaf-off and leaf-on seasons, but only during leaf-on for the deciduous species. Our results show that the evergreen species outperform both deciduous species during the leaf-on season,

intercepting over half the rainfall falling on their canopies. Bigleaf maples, on average intercepted just a little less than half the incident precipitation, while red alders intercepted a little over a third of rainfall.

During leaf-off, both evergreen species intercept a little over half the incident precipitation on their canopies, lower interception rates than their leaf-on equivalents. This difference in interception rates despite no change (or little change) in canopy cover for the evergreens between seasons is due to the fact that rainfall patterns are different in leaf-off and leaf-on seasons. Differences in rainfall intensity, intermittent dry periods, total event rainfall, are contributing factors for the difference in interception rates for the evergreen species between leaf-off and leaf-on seasons.

Transpiration: Our results showed that deciduous trees have the highest transpiration rates compared to the evergreen. Bigleaf maple species had the greatest observed leaf-on[2] transpiration – transpiring over 2/3 of the water incident on their canopies, followed by red alder. Transpiration for all species during leaf-on was strongly correlated with vapor pressure deficit. Days with high vapor pressure deficit are naturally most abundant during the summer leaf-on seasons. However, evergreen species continued transpiration during the wet leaf-off season at lower levels when vapor pressure deficits conditions were at their lowest. We did not quantify transpiration for the deciduous species during the leaf-off season, but our data suggest some transpiration does occur and further work is needed to understand those data.

Recommendations: Of the four species studied, the two evergreen species offer the most benefit to stormwater management. Red alder trees with smooth barks saw the greatest generation of stemflow, however, stemflow constituted less than 1% of the total rainfall incident on the canopy.

---

[2] Leaf-on: May to October | Leaf-off: November to April

5. References

Adams BJ, Papa F. 2001. Urban stormwater management planning with analytical probabilistic models. Canadian Journal of Civil Engineering. 28(3):545.

Allen RG, Walter IA, Elliott RL, Howell TA, Itenfisu D, Jensen ME, Snyder RL. 2005. The ASCE Standardized Reference Evapotranspiration Equation. American Society of Civil Engineers.

Anderson DB. 1936. Relative Humidity or Vapor Pressure Deficit. Ecology. 17(2):277–282. doi:10.2307/1931468.

Asadian Y. 2010. Rainfall Interception in an Urban Environment. :93.

Asadian Y, Weiler M. 2009. A New Approach in Measuring Rainfall Interception by Urban Trees in Coastal British Columbia. Water Quality Research Journal. 44(1):16–25. doi:10.2166/wqrj.2009.003.

Balian EV, Naiman RJ. 2005. Abundance and Production of Riparian Trees in the Lowland Floodplain of the Queets River, Washington. Ecosystems. 8(7):841–861. doi:10.1007/s10021-005-0043-4.

Bamber RK. 1976. Heartwood, its function and formation. Wood SciTechnol. 10(1):1–8. doi:10.1007/BF00376379.

Berland A, Shiflett SA, Shuster WD, Garmestani AS, Goddard HC, Herrmann DL, Hopton ME. 2017. The role of trees in urban stormwater management. Landscape and Urban Planning. 162:167–177. doi:10.1016/j.landurbplan.2017.02.017.

Budburst. 2022. Budburst: An online database of plant observations, a citizen-science project of the Chicago Botanic Garden. Glencoe, Illinois. [accessed 2022 Mar 8]. https://budburst.org/.

Carlyle-Moses DE, Livesley S, Baptista MD, Thom J, Szota C. 2020. Urban Trees as Green Infrastructure for Stormwater Mitigation and Use. In: Levia DF, Carlyle-Moses DE, Iida S, Michalzik B, Nanko K, Tischer A, editors. Forest-Water Interactions. Cham: Springer International Publishing. (Ecological Studies). p. 397–432. [accessed 2020 Jun 27]. https://doi.org/10.1007/978-3-030-26086-6_17.

DNR. 2022. Washington Geologic Information Portal. Geologic Units 24K. [accessed 2022 Mar 8]. https://geologyportal.dnr.wa.gov/.

Duque LF. 2020. IETD: Inter-Event Time Definition. https://cran.r-project.org/web/packages/IETD/index.html.

Duursma RA. 2015. Plantecophys - An R Package for Analysing and Modelling Leaf Gas Exchange Data. PLOS ONE. 10(11):e0143346. doi:10.1371/journal.pone.0143346.

Earle CJ. 2021. The Gymnosperm Database. [accessed 2022 Mar 7]. https://www.conifers.org/.

Ecology. 2016. Phase I Municipal Stormwater Permit. Appendix 9 – Stormwater Discharge Monitoring. Olympia, WA. [accessed 2021 Nov 28]. https://ecology.wa.gov/Regulations-Permits/Permits-certifications/Stormwater-general-permits/Municipal-stormwater-general-permits/Municipal-Stormwater-Phase-I-Permit.

Feau N, Mcdonald M, Van Der Meer B, Zhang Y, Herath P, Hamelin RC. 2022. Phytophthora species associated with red alder dieback in British Columbia, Canada. Canadian Journal of Plant Pathology. 0(0):1–10. doi:10.1080/07060661.2021.2022763.

Gebauer T, Horna V, Leuschner C. 2008. Variability in radial sap flux density patterns and sapwood area among seven co-occurring temperate broad-leaved tree species. Tree Physiology. 28(12):1821–1830. doi:10.1093/treephys/28.12.1821.

Granier A. 1985. Une nouvelle méthode pour la mesure du flux de sève brute dans le tronc des arbres. In: Annales des Sciences forestières. Vol. 42. EDP Sciences. p. 193–200.

Hanson B, Orloff S, Peters D. 2000. Monitoring soil moisture helps refine irrigation management. California Agriculture. 54(3):38–42.

Hartmann DL. 1994. Global Physical Climatology. Academic Press.

Hillis WE. 1968. Chemical aspects of heartwood formation. Wood Science and Technology. 2(4):241–259. doi:10.1007/BF00350271.

Hummel SS. 2009. Branch and crown dimensions of Douglas-fir trees harvested from old-growth forests in Washington, Oregon, and California during the 1960s. Northwest Science. 83(3):239–252.

Ishii HR, Sillett SC, Carroll AL. 2017. Crown dynamics and wood production of Douglas-fir trees in an old-growth forest. Forest Ecology and Management. 384:157–168. doi:10.1016/j.foreco.2016.10.047.

Klinka K, Brisco D, British Columbia, Ministry of Forests and Range. 2009. Silvics and silviculture of coastal western redcedar: a literature review. Victoria: British Columbia, Ministry of Forests and Range, Forest Science Program.

Kuehler E, Hathaway J, Tirpak A. 2017. Quantifying the benefits of urban forest systems as a component of the green infrastructure stormwater treatment network: Quantifying the Benefits of Urban Forest Systems as Green Infrastructure. Ecohydrology. 10(3):e1813. doi:10.1002/eco.1813.

Kutscha NP, Sachs IB. 1962. Color tests for differentiating heartwood and sapwood in certain softwood tree species.

MacKinnon A, Pojar J, MacKinnon A, British Columbia, Ministry of Forests L and NRO. 2016. Plants of the Pacific Northwest coast: Washington, Oregon, British Columbia & Alaska.

Miller RE, Murray MD. 1978. The effects of red alder on growth of Douglas-fir. :26.

Minore Don. 1983. Western redcedar; a literature review. Portland, OR: U.S. Department of Agriculture, Forest Service, Pacific Northwest Forest and Range Experiment Station Report No.: PNW-GTR-150. [accessed 2020 Jul 21]. https://www.fs.usda.gov/treesearch/pubs/7680.

Murgatroyd AL, Ternan JL. 1983. The impact of afforestation on stream bank erosion and channel form. Earth Surface Processes and Landforms. 8(4):357–369. doi:10.1002/esp.3290080408.

Oishi AC, Oren R, Stoy PC. 2008. Estimating components of forest evapotranspiration: A footprint approach for scaling sap flux measurements. agricultural and forest meteorology.:14.

Oren R, Phillips N, Ewers BE, Pataki DE, Megonigal JP. 1999. Sap-flux-scaled transpiration responses to light, vapor pressure deficit, and leaf area reduction in a flooded Taxodium distichum forest. Tree Physiol. 19(6):337–347. doi:10.1093/treephys/19.6.337.

OSU. 2022. Oregon Wood Innovation Center. [accessed 2022 Mar 7]. https://owic.oregonstate.edu.

Perakis SS, Pett-Ridge JC. 2019. Nitrogen-fixing red alder trees tap rock-derived nutrients. Proceedings of the National Academy of Sciences. 116(11):5009–5014. doi:10.1073/pnas.1814782116.

Prevéy JS, Harrington CA. 2018. Effectiveness of winter temperatures for satisfying chilling requirements for reproductive budburst of red alder (Alnus rubra). PeerJ 6(13): e5221-. 6(13):e5221. doi:10.7717/peerj.5221.

R Core Team. 2021. R: A Language and Environment for Statistical Computing. Vienna, Austria: R Foundation for Statistical Computing. https://www.R-project.org/.

Ratliff LF, Ritchie JT, Cassel DK. 1983. Field-Measured Limits of Soil Water Availability as Related to Laboratory-Measured Properties. Soil Science Society of America Journal. 47(4):770–775. doi:10.2136/sssaj1983.03615995004700040032x.

Restaino CM, Peterson DL, Littell J. 2016. Increased water deficit decreases Douglas fir growth throughout western US forests. Proceedings of the National academy of Sciences. 113(34):9557–9562.

Restrepo-Posada PJ, Eagleson PS. 1982. Identification of independent rainstorms. Journal of Hydrology. 55(1–4):303–319.

Seebacher TM. 2007. Western redcedar dieback : possible links to climate change and implications for forest management on Vancouver Island, B.C. University of British Columbia. [accessed 2021 Dec 2]. https://open.library.ubc.ca/soa/cIRcle/collections/ubctheses/831/items/1.0074955.

Sillett SC, Goslin MN. 1999. Distribution of epiphytic macrolichens in relation to remnant trees in a multiple-age Douglas-fir forest. Can J For Res. 29(8):1204–1215. doi:10.1139/x99-081.

Simard SW, Durall DM. 2004. Mycorrhizal networks: a review of their extent, function, and importance. Can J Bot. 82(8):1140–1165. doi:10.1139/b04-116.

Smith DM, Jackson NA, Roberts JM, Ong CK. 1999. Reverse flow of sap in tree roots and downward siphoning of water by *Grevillea robusta*. Functional Ecology. 13(2):256–264. doi:10.1046/j.1365-2435.1999.00315.x.

Stanke H, Finley AO, Domke GM, Weed AS, MacFarlane DW. 2021. Over half of western United States' most abundant tree species in decline. Nat Commun. 12(1):451. doi:10.1038/s41467-020-20678-z.

Taubenhaus JJ, Ezekiel WN, Lusk JP. 1931. Preliminary Studies on the Effect of Flooding on Phymatotrichum Root-Rot. American Journal of Botany. 18(2):95–101. doi:10.2307/2435932.

USFS. 2022. Fire Effects Information System. [accessed 2022 Mar 8]. https://www.feis-crs.org/feis/#.

Waring RH, Franklin JF. 1979. Evergreen Coniferous Forests of the Pacific Northwest: Massive long-lived conifers dominating these forests are adapted to a winter-wet, summer-dry environment. Science. 204(4400):1380–1386. doi:10.1126/science.204.4400.1380.

Weil RR, Brady NC. 2016. The nature and properties of soils. Fifteenth edition. Columbus: Pearson.

Wilson KB, Hanson PJ, Mulholland PJ, Baldocchi DD, Wullschleger SD. 2001. A comparison of methods for determining forest evapotranspiration and its components: sap-flow, soil water budget, eddy covariance and catchment water balance. Agricultural and Forest Meteorology. 106(2):153–168. doi:10.1016/S0168-1923(00)00199-4.

WSU. 2022. PNW Plants. [accessed 2022 Mar 7]. http://www.pnwplants.wsu.edu/.

Appendix A – Methods

Soil Moisture Probes and Canopy VPD Sensors

    a) Soil Moisture Probes:

Probes were distributed near study trees located at each of the four cardinal directions around one center probe at the data logger. Soil moisture probes were installed 5 per plot at a depth of 12 to 18 inches depending on root structure and soil type. The nearest study tree to each soil moisture probe was noted. When evaluating soil moisture readings, the proximity to the nearest tree and composition of overhead canopy was considered.

Plots 7 and 8 (Webster) were located on a flood plain consisting of loose aggregate and cobble mixed with sandy soil. It was difficult to install these probes at depth and the measurements recorded at these sites were susceptible to inundation during the rainy season. In general, a reading of greater than 40% soil moisture was associated with standing water. Observations of standing water suggests soil saturation, at which all pores are filled with water, and occurs at a range of volumetric water content values from 30 to 60% for sandy to clay soils (Weil and Brady 2016).

As stated, the aim of soil moisture measurements was to assess general soil conditions that may impact tree water availability for transpiration. Patterns of soil wetting associated with throughfall from rain events were also of some interest but was not intended to be thoroughly evaluated. No effort was taken to further quantify soil properties such as soil type, water potential, hydraulic conductivity, nutrient levels, or organic carbon content. Therefore, it is important to note that without additional context, soil moisture results should be considered semi-quantitative at best.

While soil saturation is one important consequence of winter flooding, tree health and water-use are not likely to be adversely impacted by a short-term excess of soil water. This is especially true of the native trees studied which may be adapted to such environments and have relatively low metabolic requirements during winter months. Two exceptions would be root-rot from sustained inundation (Taubenhaus et al. 1931) and tree fall from bank erosion (Murgatroyd and Ternan 1983), neither of which was observed for the study trees. More importantly, low soil moisture during prolonged summer droughts has the potential to limit water-use via transpiration. While it was not a study objective to properly determine the field capacity and permanent wilting points of the plot soils, it was expected that volumetric water content values below 10 to 15% increasingly resulted in drought stress. The permanent wilting point, at which trees are no longer able to absorb water through their roots, ranges from 4 to 22% volumetric water content, in sandy to clay soils

respectively (Ratliff et al. 1983; Hanson et al. 2000). Soil at both sites is Pleistocene continental glacial till with a mix of sand, silt, and clay, but with higher clay content and greater compaction at Evergreen and higher sand and silt content and increasingly well-sorted alluvial gravel depositions near the bed of salmon creek Webster (DNR 2022). Therefore, it is likely that the volumetric water content associated with permanent wilting point is slightly higher at Evergreen and that neither site represents an extreme for soil composition.

Among all groups of sensors deployed for this study, soil moisture probes proved to be the least reliable. In many cases, sensors failed after water penetrated the mote's weatherproofing and corroded the data loggers circuitry. In other cases, data were determined to be unreliable when plotted and thereby abandoned. However, of the five probes originally deployed per plot, at least two per plot were able to provide a continuous data stream during the study duration. Measurements from capacitance probes were supplemented by time-domain reflectometry (TDR) probes deployed part way through the study to provide quality assurance.

  b) Canopy VPD Sensors:

Canopy VPD sensors measured relative humidity (RH) and air temperature (atmospheric pressure measured by weather stations) and were hung at approximately half canopy height for 5 canopies covering the 8 plots. Trees selected for canopy VPD sensors were not necessarily study trees, rather, suitable branches were chosen near the mid-points of each stand.

Sensors were hung using an arborist throw bag attached to a line and tossed over an exposed branch at height. The line was secured to the respective tree trunk, but it was difficult to retrieve these sensors after seasonal epiphyte growth secured the line to the tree branch. In most cases, the solar panel was sufficient for maintaining a data stream throughout the study. Some data loss near the end of the study was filled by a well-established relationship between these sensors and weather station measurements.

Data from these sensors were processed using the plantecophys package in R (Duursma 2015). Put simply, VPD represents "the strain under which an organism is placed in maintaining a water balance during temperature changes" (Anderson 1936) and is calculated in Equation 1 (Hartmann 1994; Allen et al. 2005).

$$Saturation\,Vapor\,Pressure\,(e_s) = \; 0.611 \; \times exp\left(\frac{L}{R_v} \times \left(\frac{1}{273} - \frac{1}{T+273}\right)\right)$$

$$Saturation\ Vapor\ Pressure\ (e_a) = \frac{RH}{100 \times es}$$

$$Vapor\ Pressure\ Deficit\ (VPD) = e_s - e_a$$

Equation 1: Vapor pressure deficit calculation.

Where, $L = 2.5 \times 10^6\ JK^{-1}kg^{-1}$ (latent heat of vaporization); $R_v = 461\ JK^{-1}kg^{-1}$ (the gas constant for water vapor), T is the air temperature (°C) and RH is the relative humidity (%).

Qualifying Storm Events

Definitions and Criteria:

a) **Storm Node:** 15-minute resolution timestamp associated with storm start or end.

b) **Inter-Event Dry Period:** 6 hours. Length of rolling window for which a storm node is created if cumulative precipitation drops below the minimum rain depth.

c) **Minimum Rain Depth:** 0.5 mm. Accumulated rain depth which triggers node creation within the rolling window.

d) **Minimum Storm Depth:** 5 mm. Total rain depth required for a valid storm.

e) **Minimum Storm Duration:** 2 hours. Amount of time between nodes required for a valid storm. Note that Ecology does not have a fixed minimum or maximum, however, storms less than 2 hours were extreme outliers requiring a minimum storm intensity of 2.85 mm/hour. These storms were removed for quality assurance purposes and to ensure data integrity.

f) **Antecedent Dry Period:** 24 hours. Amount of time between two individual storms. Note that Ecology expands these criteria to 48 hours for dry season storm events. Since the dry season for the Phase I Municipal Stormwater Permit does not align with leaf-on/leaf-off definitions this expansion was ignored. Use of the 48-hour definition would also severely limit the sample size of leaf-on storms which are already limited in comparison to leaf-off storms. The intention of this Ecology criteria is to maximize the "first flush" effect for chemical sampling which is not applicable to this study.

g) **Post-Storm Drip Period:** 5.5 hours. Amount of time after storm cessation to expand the storm for measuring throughfall to account for canopy drip-through.

Interception Estimates

Throughfall

Thirty-eight trees were instrumented for the measurement of interception using throughfall troughs. Two throughfall transects per tree canopy were sampled using methodology from Asadian et al. (2009; 2010). Throughfall measurements were normalized by the combined trough surface area and aggregated over a storm to arrive at a throughfall depth estimate. These throughfall depth values were subtracted from precipitation depths recorded by rain gages set up in the open – or open canopy readings. The resulting "interception depth" when expressed as a fraction of total storm precipitation depth gives the fraction of rainfall intercepted by the tree's canopy during that storm event. If desired, this ratio can then be applied to the tree's canopy area for creating individual tree water budgets.

In practice, a tree's canopy is rarely uniform in shape and often overlaps with the canopies of nearby trees. This is especially true of the more natural areas where residual stands of mature native trees are typically found. In this study, several practical concessions were made as detailed in the methods below.

Throughfall troughs were made from 4-inch Charlotte Pipe PVC schedule 40 DWV irrigation pipe. Each section of pipe was nominally 10 feet in length but measured approximately 10.625-feet (120 5/8-inch or 300 mm). Three slits measuring 33 1/3-inch in length were cut in even intervals throughout the length of the pipe with 10-inch gaps between openings.

A rain gauge with a diameter of 6.5-inch was installed at the point of intersection of the two pipes so that water collected by the troughs pour into this rain gage. The rain gauge was covered with a flexible nylon mesh netting to prevent debris from clogging the gauges. A nominal mesh size of 1 mm (18-mesh) was determined to prevent the most debris while allowing rainfall to pass through unabated by surface tension (which decreases with temperature; potentially biasing measurements). Rain gauges were still frequently clogged with smaller conifer needles, pollen, and dust thus requiring regular maintenance.

Four considerations were made when establishing transects for trough placement (in order of importance):

a) **Physical obstructions.** Since t-posts were used to secure trough anchors, it was necessary to avoid rocks, roots, and other physical obstructions that made such installations impossible.
Troughs were aligned in a way that allowed them to both meet at the rain gauge on their downslope facing ends. This meant that troughs could not be placed on either side of the tree bole and could not be placed at an exceptionally acute or reflexive angle (~< 30° or ~> 240°).
Five-foot t-posts were utilized on either end of the troughs and were inserted to depths of 6 to 12-inches (depending on soil type). Rain gauges were installed at one-foot from the ground level to limit interference from grassy overgrowth and prevent insects from accessing the drain slot.

b) **Canopy overlap.** While mostly dominant trees were chosen for the study, canopies often tended to intersect vertically. Particularly stratified canopy structures were observed at Webster South Field and Evergreen Organic Farm. In these cases, Douglas-fir tended to dominate the overstory canopy layer with canopy density increasing at height (Bingham and Sawyer 1991) and sprawling bigleaf maple occupying the understory. When placing troughs care was taken to avoid sections of canopy overlap.

c) **Canopy dripline.** Intercepted precipitation may be redirected to the stem and dripline. For solitary trees, the dripline is somewhat well defined as the canopy's edge where throughfall is concentrated. For more complex systems with overlapping canopies, the dripline is much more difficult to spatially quantify. It was also difficult to place troughs in a way that captured the dripline and avoided other canopies or

42

open space. Instead, we thought of the dripline as less of a two-dimensional feature and more of a gradient. Trough lengths were chosen to be 10-feet consistently as a matter of practicality, but this also allowed for a conservative approach since individual tree canopies were rarely less than 10-feet in radius in any direction. When given the choice, sections of uneven lateral growth were avoided and transects where the dripline was approximately 10' from the bole were prioritized.

d) **Randomization.** When not fully limited by the above considerations, transect bearings were randomly determined. In the northern hemisphere tree canopies tend to be concentrated facing south where the sun's angle provides a greater exposure to photosynthetically active radiation. To avoid potentially biasing the data, transects were placed at either consistently selected specific bearings straddling 180° (e.g. 150° and 210°) or at randomly chosen bearings. Since consistent placement was not feasible, the latter calculation was performed when applicable.

Rainfall Calibration

Weather Station Rain Gauges

An open canopy trough system was installed at Webster on September 20, 2020, to more accurately determining the calibration coefficient used to normalize throughfall troughs. Prior analyses normalized throughfall data using only the nominal slit area to determine the ratio between the effective surface area of the throughfall troughs and the weather station rain gauges. The point of creating an in-situ comparison between open and closed canopy troughs was to account for the unique characteristics of the trough systems.

Rain Gauge Offsets

Onset Davis rain gauges were factory calibrated and subsequently field calibrated for throughfall collections in late February 2020. Field calibration was performed using a rain gauge calibration kit (FCD-653, Hydrological Services) to pass 653 mL of water at 100 mm/hour through each rain gauge and record the number of tips. Excess water left in the gauge's tipping mechanism was measured with a syringe and added to the total.

Field calibration errors were rectified with an offset ratio directly applied to raw data. For the rain gauges, which have a catch area of 16.5 mm (funnel opening diameter), ~120 tips (0.254 mm per tip) were expected. In general, field calibration resulted in far fewer tips being recorded (typically 90-100 tips). This suggests that these rain gauges were under-tipping in the field and a positive offset ratio was applied on a trough specific basis.

Field calibrations were also recorded for weather station rain gauges after the conclusion of the study (as to not interfere with storm calculations). These rain gauges also undertipped at 91 and 99 tips for Evergreen and Webster respectively. This equates to correction factors of ~1.3x and ~1.2x respectively.

At Webster, corrected storm totals were compared to an adjacent meteorological grade weather station (installed on October 20, 2020). This weather station is maintained and operated by AgWeathernet and sponsored by the DNR Webster Forest Nursery frost prevention program. Rain gauges were placed at a lower altitude and wind shielded, but otherwise provided a high-accuracy comparable data stream for QA/QC purposes.

A regression (n > 50) model was developed between the meteorological grade rain gage and our rain gage to determine a potential scaling factor. The model indicated that the offset ratio of 1.2x was appropriate for Webster.
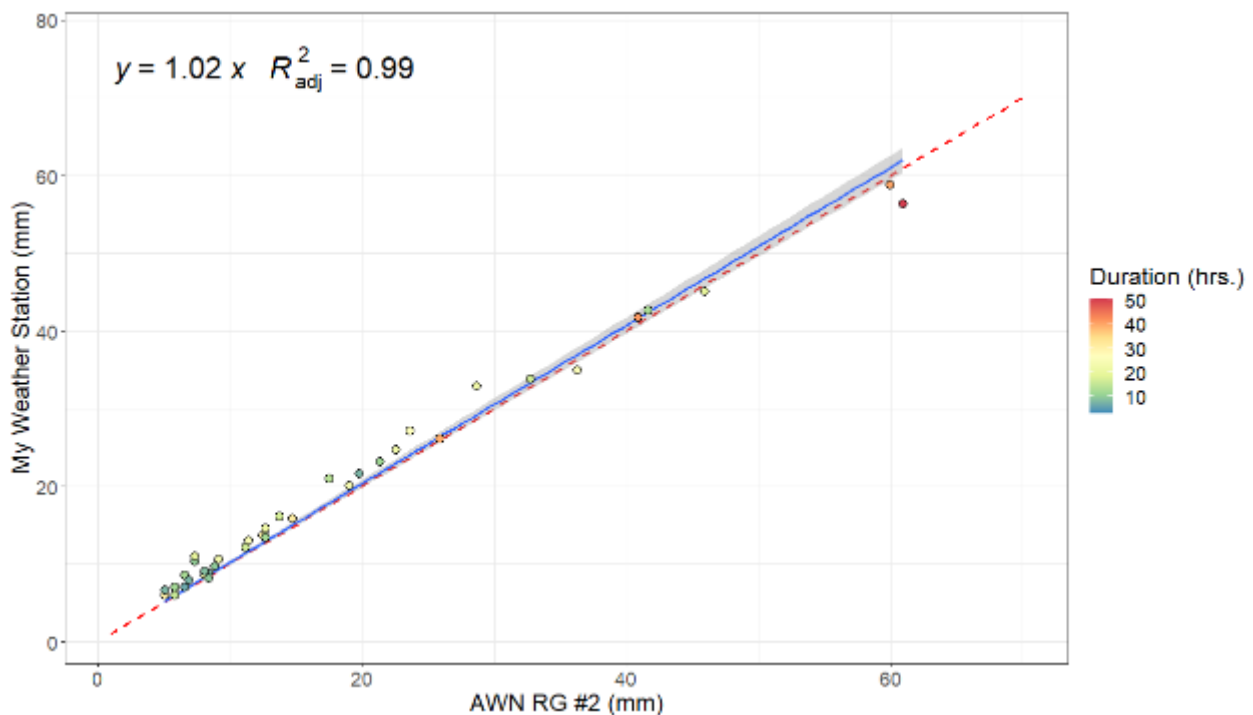
Figure A14: Regression relationship between calibrated Webster weather station rain gauge data and a nearby tier-1 weather station.

Censoring

Some measurements had to be excluded due to clogging of the rain gage. Rain gage clogging was identified by visual inspections and when the data showed a characteristic infrequent but regular tipping – a signature of a clogger rain gage.

Figure A15: A rain gauge clogged with dirt and pollen which was able to penetrate the protective mesh covering.

Trough Slits

Three slits per trough were cut to the nominal dimensions 1-1/2 by 33-1/3-inches based on the methodology used by Asadian (2010). PVC tended to bow while cutting meaning that the middle was often narrower. To compensate for these irregularities trough measurements were made and a correction factor was applied to the dataset using the surface area of the slits for open-canopy system to normalize throughfall.

To assess the surface area of the troughs, a series of top-down photos was taken with a smart phone (Samsung ISOCELL 2L4 (S5K2L4) CMOS camera sensor). Before image acquisition, several pieces of information were noted on the trough: a) tree id; b) replicate (left/right); c) degree of slope; d) two-inch demarcations from up and down gradient slit edges for scale. Each photo showing the extent of the trough, was analyzed, and corrected for angular and spherical distortions in Adobe Photoshop CC 2022.

Canopy Cover

Two images were taken facing upwards aligned with each trough using a Samsung Galaxy S10 phone. A bubble level mounted on the phone was used to level the phone horizontally and the image was centered at the mid-point of each trough.

Measurements for % canopy cover were made by manually applying a threshold gate to each image in Adobe Photoshop CC 2022. This converted each RGB image to the HSV color space and then to a black/white bitmap assigning each pixel a value of 0 (black) or 255 (white). The threshold was scaled to convert high-value (bright) pixels representing the sky (background) to white and lower-value (dim) pixels representing the canopy (foreground) to black. Due to automatic camera adjustments made to compensate for changing background light conditions, this process had to be done separately for each image. The process was semi-automated using an image histogram to determine the mean value of sky pixels, which was usually identified by a right-skewed blip in the left-skewed distribution (Figure A1613).

After thresholding, an elliptical mask was centered on the image and the number of black and white pixels were compared to determine % canopy cover.

Figure 16A: Example of an appropriate threshold value based on a noticeable bump in the histogram from the number of sky pixels.

Figure 16B: An elliptical mask applied around the center of the canopy image.

Throughfall Calculations

Rain gauge measurements associated with throughfall troughs were processed into 15-minute intervals. For each qualifying storm event, throughfall measurements were tabulated. In the storm definitions, an extra 5.75 hours (< 6 hour IETD) was added to the end of each event to allow for continued collection of throughfall representative of canopy drip. Throughfall totals were compared against weather station storm totals and percent

throughfall was calculated. In order for this comparison to be appropriate several transformations were applied:

a) **Rain Gauge Offsets.** As with the weather station rain gauges, throughfall rain gauges also tended to under-tip. An calibration offset was calculated and applied to raw throughfall data.

b) **Weather Station Normalization.** A co-efficient derived from comparing an opening canopy system at Webster to weather station rain gauge data was applied to all throughfall troughs. This accounted for the difference in surface area between troughs and rain gauges in addition to a host of other possible parameters/interactions.

c) **Trough Measurements.** The difference in surface area between each under-canopy throughfall system and the open canopy system at Webster was calculated and applied as trough factor.

Select throughfall storms were also censored (excluded) from the data if field notes indicated that the rain gauge had been clogged. Clogs and other data anomalies were also identified automatically using the following criteria. The complexity of these criteria underscore the nuances of continuous throughfall data collection.

a) **Low Throughfall.** The minimum storm event criteria specifies 5 mm of open canopy rain fall. Since this is the equivalent of ~ 44 mm of throughfall after weather station normalization, it is expected that any given storm event should generate quantifiable throughfall. This should, in theory, hold true even for low intensity events since the minimum tip measurement of 0.254 mm is the equivalent of ~0.5% throughfall. Therefore, less than four tips (2%) throughfall during the storm duration (including drip period) was an indicator of a potential clog. Additionally, measurements less than 5% were also excluded if rainfall depth exceeded 10 mm.

b) **Extended Drip Period.** While clogs typically obstructed the passage of any rainfall through the gauge it was also common to see evidence of a partial clog in the data. Generally, this happened when the trough's funnel spout was narrowed by debris to the extent that rainfall was not allowed to pass through the gauge at the rate required to prevent an accumulation of water within the rain gauge catch. If water was still able to clear the catch within the normal drip period this phenomena was indistinguishable from canopy drip and did not present an issue for analysis of total throughfall.

If episodic dripping continued to be detected after the canopy drip period, this throughfall was not included for the preceding storm and represented a data integrity issue that biased the collection to under-reporting throughfall. To identify such instances and exclude them from the dataset an extended drip period was created to 12-hours post-storm. The default drip period (5.75 hours) was intended to avoid conflicts with adjacent storms by being set to less than the IETD window (less than 0.5 mm in 6 hours). As a result, a 12-hours period was expected to overlap with some subsequent storms, however these storms did not qualify as they were excluded using the 12-hour ADP filter. Therefore, the previous storm was invalidated based on the extended 12-hour drip period:

i) If no weather station rain gauge measurements were detected and accumulated throughfall measurements exceeded 1 mm (4 tips), OR

ii) If a subsequent storm or additional open-canopy rainfall was detected and throughfall values exceeded 120%.

c) **High Intensity.** Rain gauges were specified to within 5% accuracy for precipitation rates of up to 100 mm/hr. While this accuracy was not observed in-situ data was flagged when raw precipitation rates exceeded 120 mm/hr (adding in a buffer). Additionally, 15-minute intensity measurements greater than 2x weather station values were flagged. Flagged data was then analyzed visually (as detailed below) to determine if the event was to be excluded. This was done using two semi-automated criteria since high intensity values were rare in the dataset. The event was censored if:

i) Several high intensity measurements (over 120 mm/hr) were detected that would significantly degrade the overall accuracy of the event (influential points determined with tf_total_mm ~ wx_mm within a one-hour rolling window where Cook's Distance > 4/sample size).

ii) Intensity (as determined as the derivative [tangent] in the profile analysis described below) did not match the weather station profile indicating that a clogged bit was freed during the storm resulting in a flood of storm from the trough.

d) **Profile Analysis.** Individual storm profiles were plotted and analyzed visually for odd patterns in precipitation that could not be explained by the weather station profile. This process was semi-automated deploying several statistical tests to help assess time series trends.

Workflow

- Read raw stemflow data using a flatfile from data logger export.

- Determine correction factors for trough measurements, rain gauge calibration, and weather station calibration.

- Add in tree metadata to link rain gauge serial numbers to tree IDs.

- Separate out data from the parking lot, based on tree ID, and apply a separate weather station calibration factor that does not include the trough's surface area.

- Merge with rainfall data for qualifying storm events from the weather stations.

- Filter out censored data.

- Adjust throughfall values to the same basis as weather stations.

- Calculate throughfall for each storm event.

Stem Flow

<u>Installation</u>

Stemflow was measured by affixing collars to 12 trees at each site (24 trees total) beginning in January 2020. Bark surrounding each collar was shaved. Collars were made from a polyurethane foam (DuPont Great Stuff) cast around petroleum jelly (Vaseline) coated tubing and coated with a hydrophobic sealant (Flex Seal). This created a channel to direct stemflow to a tube secured with marine sealant (Aquaseal) following a single helical rotation of the collar around the tree bole. Water was transferred from the tubing to a four-gallon bucket placed at the base of each tree. The contents of the buckets were routinely emptied, and the volumes of water decanted from them recorded.

Stemflow collection volumes were recorded in mL for each collection event. One-liter graduated cylinders, with 10 mL precision, were used for smaller collections. Larger collections (over 1 L) required multiple measurements with a graduated cylinder compounding error. A hanging scale with 0.02 kg (20 mL) precision was used with larger collections.

<u>Data Analysis</u>

Each stemflow collection was made opportunistically to target dry periods between storms. As a result, multiple qualifying storm events were often captured within a single stemflow collection. Stemflow volumes were converted to percentages using the total amount of qualifying rainfall between collections. Two stemflow ratios were calculated by applying the total rainfall depth to the surface areas of the tree's:

a) **Canopy:** Percentage of canopy interception as the fraction not accounted for by throughfall which is redirected to the tree's main stem.

b) **Stem:** The stem funneling ratio as the fraction of water directly interacting with the tree's basal footprint.

Both ratios are hydrologically significant, however, only the percentage of canopy interception is directly comparable to throughfall measurements. The importance of the stem funneling ratio is related to tree canopy morphology. A value greater than one indicates that stemflow is not simply a product of the tree bole. The influence of the greater canopy is expected to be greatest for trees with sprawling canopies and upward sweeping branches. These canopy features tend to conduct water to the main stem rather than the canopy drip line.

<u>Workflow</u>

- Read raw stemflow data using a flatfile created from the field collection form.
- Filtered out all "NAs" from partial and omitted collections.
- Merged in qualifying storm data by expanding the time between collections into a continuous time series.

- o Note that qualify storms for stemflow did not require a minimum ADP and did not specify a maximum duration or rainfall depth. It is also important to note that the end date/time of this storms did not include a drip period since this concept is only applicable for continuous throughfall collections.
  - o By only counting qualifying storm precipitation between collections we are making the assumption that ambient rainfall (not associated with a storm) does not generate stemflow. By the IETD framework, this would be any rainfall that does not accumulate to at least 0.5 mm in a rolling 6-hour window.
- Summed total qualifying precipitation between collections and summarized storm characteristics.
- Filtered out collections without any qualifying precipitation in addition to overfilled data (right-censored collections).
- Added in seasonal delineation (May to October: Leaf-On; November to April: Leaf-Off).
- Created grouped tree IDs for multi-stemmed canopies.
- Calculated combined stemflow volumes for multi-stemmed canopies only if both stems were measured as valid collections.
- Calculated the percent interception using the canopy area for each canopy and the stem funneling ratio using the basal area for each stem.

Uncertainty

- **Overflow:** Initial research on stemflow indicated that very little stemflow would be generated by larger trees and it was determined that a 4-gallon collection vessel would be appropriate. While this was the case for most storm events and trees, several large storm events overfilled the collection vessels. These collections were right-censored (> 15 L) in the dataset and were removed from subsequent analyses.

- **Clog and Leaks:** It was often difficult to determine whether a low stemflow collection after significant precipitation was the result of an issue with the stemflow system. Debris stuck in the collar or tubing was cleaned out during collections and some repairs were made to weathered seals. When significant issues were found the collection was censored from the dataset. Generally, there were few obvious issues with the notable exception of 4-8-DF which lost a significant amount of its collar from an adjacent tree fall in early 2021 and was not able to be repaired.

- **Other Considerations:** Several environmental factors that may impact stem flow were not able to be quantified and should be noted:

a) Many trees in the study had rich epiphyte communities (mosses) above the stemflow collars which could capture stemflow. Since mosses were also present below the stemflow collars, it is also possible that some of the stemflow measured would have been intercepted.

b) Each stemflow collar was constructed around natural features of each tree including knots, growths, and other small obstructions. This, in addition to the difficulty of even foam application, was the source of some variability in channel width, slope, and placement height.

c) As with throughfall, this study assumes that rain falls vertically and is not swept by the wind during storms. It is also assumed that rain falling directly on the stem flow collars can be counted as stem flow since the collars did not typically extend from the tree bole more than ~1-2 inches.

Transpiration by Sap flux

Installation

Sap flux was measured using the thermal dissipation probe (TPD) method as first described by Granier (Granier 1985). TDP systems were manufactured by DynaMax Inc. (**cite reference manual**) and consisted of a data logger (Campbell Scientific CR-1000X), an adjustable voltage regulator (AVRD), and several types of probes capable of measuring sap flux at a variety of depths (15, 25, 50, 70, and 90 mm).

Two cylindrical probes, 1.75 mm in diameter, were inserted radially into parallel holes drilled 40 mm apart vertically in the tree's xylem. Four lengths of probes were used in the study, 30, 50, 80, and 100 mm, providing measurements at 15, 25, 15 and 70, and 15, 50, and 90 mm respectively. All 64 trees in this study were measured at more than one depth using a combination of probes.

The upper probe was supplied a constant voltage and was continuously heated while the bottom probe, unaffected by the heat, provided reference measurements. The difference in temperature between the upper and lower prong (ΔT or dT) was sampled every minute and recorded as 15-minute averages.

Data Gaps

During the two years of data collection, several logistical issues prevented collection of un-interrupted continuous TDP data. These were to be expected some redundancy was incorporated into the study plan to address this.

Data Processing

As the tree transpires, the rate of water movement through the main stem increases and the heated top probe is cooled. As a result, the difference in temperature between the two probes decreases. To calculate sap flux via the Granier method, it is typically assumed that there is a point of zero sap-flux every 24-hours and that this is observed as the local maxima of dT. Each subsequent observation for a 24-hour cycle is then normalized by dTMax and the dimensionless "flow index", K, is ccompued. While dTMax is often assumed to be constant for each 24-hour period, this assumption results in a sudden change in sap flux as dTMax shifts. To address this issue, dTMax was interpolated with a continuous linear approximation based on the methodology from Baseliner for MATLAB (Oishi 2016).

$$K = \frac{\Delta T_m - \Delta T}{\Delta T}$$

To calculate sap flux, the Granier equation includes two empirical coefficients where α = 0.0119, β = 1.231, and F is sap flux in cm^3 of water per cm^2 of sapwood per second.

$$F = \alpha \times K^{\beta}$$

Uncertainty

The Granier method makes two important assumptions:

a) Nighttime sap flux is negligible meaning that pre-dawn dTMax can be used to calibrate zero sap flux.

This assumption is critical to under-pinning of the Granier method. Several studies have suggested this to be one important factor for TDPs under-estimating transpiration compared to other methods such as Eddy Covariance (Oren et al. 1999; Wilson et al. 2001; Oishi et al. 2008).

b) Sap flux moves in one direction, up the tree, and the tree does not move water from the crown to the roots.

The two probe TDP setup is not able to accurately measure "reverse sap flux" and the sap flux rate is always greater than or equal to 0. Any reverse sap flux in or data set would be indistinguishable from dTMax estimates.

From a physiological perspective, certain tree species are capable of reverse sap flux or downward siphoning of water (Smith et al. 1999). This should only be an issue under specific conditions when vapor-pressure deficit is low, and the soil is well saturated. Otherwise, the water potential of the tree's capillary system should be greater than gravitational potential. In our study, the lowland species, red alder, is the most susceptible to this phenomenon.

Sapwood Area

For many conifers, including Douglas-fir (*Pseudotsuga menziesii*) and western redcedar (*Thuja plicata*), the boundary between wet sapwood and dry heartwood is often determined visually. The sapwood boundary, which may be observed and measured using a sample obtained from an increment borer, occurs at the transition between light and dark wood (Kutscha and Sachs 1962). Lighter sapwood is indicative of elevated water content and intact pores within tracheids while darker heartwood is rich with tannins and resins making it far less hydraulically active (Hillis 1968; Bamber 1976).

In Douglas-fir, when the sapwood transition was not obvious, the core was exposed to a pH indicator solution (bromcresol green) which is sensitive to the hydrogen-activity of phenolic compounds present in heartwood. The same pH indicator solution was ineffective at highlighting sapwood in western redcedar or either of the deciduous tree species. In difficult cases, western redcedar samples were stained with Benedict's solution (Minore 1983). However, in most western redcedar samples taken, the transition was obvious without the need for a stain.

In the photograph below, a Douglas-fir core is being measured for sapwood area. The extent of the blue/green stain is indicative of sapwood. Earlywood rings, which are more porous, absorbed a greater amount of dye creating a striped appearance. When this resulted in the sapwood boundary being located at the edge of an earlywood to latewood transition the latewood midpoint was used. This difference was typically less than 2 mm.

Figure A17: Bromocresol green stained sapwood in several Douglas-fir core samples.

For the deciduous species in this study, including bigleaf maple (*Acer macrophyllum*) and red alder (*Alnus rubra*), the transition between sapwood and heartwood is less visually obvious due to the complexity of their vascular tissue anatomy. To properly assess sapwood depth in deciduous species it was necessary to use a variety of different techniques including a tracer dye method (Gebauer et al. 2008).

A 0.1% solution of indigo carmine solution was injected into a hole, created with a 1/16" diameter drill bit to a depth of ~ 300 mm, at breast height (1.3 m) in the morning during a sunny day when transpiration was expected to increase. After several hours, a core sample was taken at 3 to 5 cm above the dye injection port and the stained depth was used to estimate the sapwood depth. In the field, the tracer dye method was difficult to successfully implement since it required the increment bore sample to be taken directly above and parallel to the hole.

Ultimately, this technique confirmed a suspicion that most of our deciduous trees had sapwood at depth, often extending nearly to the pith. Since the dye tended to fade near the supposed sapwood boundary, it was not possible to use this technique to determine the sapwood depth with the same precision as conifers (1 mm). Rather, observations from the dye injections were paired with attenuation patterns to estimate the sapwood depth with 5 mm precision.

Attenuation

Sap flux data provide an estimate of the rate at which water is moving up the tree at specific depth. A single measurement can be applied to a band of sapwood to calculate the volume of water transported by the tree per day. However, sap flux does not remain constant

throughout the radial sapwood profile. By taking measurements at multiple depths, an attenuated sap flux profile can be constructed to more accurately assess whole tree water-use. In this study, linear interpolation was used to estimate sap flux between measured depths. When sapwood depth extended past the furthest measurement depth an exponential decay function was used to interpolate the remaining values.

Censoring and Data QC

While TDPs are considered a robust and reliable method for measuring sap flux it is important to recognize data that may be compromised by electrical issues. These data should be censored and removed from the dataset since they do not reflect actual sap flux. Considering the frequency of measurements, number of probes and wires, need for constant power, and harsh environmental conditions it was expected that some significant portion of the dataset would need to be censored.

Censoring TDP data was mostly a manual process. Most data issues were observed through time series plots of raw data using Campbell PC400 during data collection. Additionally, a semi-automated routine flagged potentially problematic data during processing. dT is typically within the range of 2 to 20 °C and TDP data outside of this range were flagged. Data were also flagged if the slope between measurements exceeded 1 which was often observed with wiring issues. All flagged observations were then plotted to manually determine the potential cause and extent of the data issue.

The most common cause of erroneous TDP data was corrosion caused by water penetrating the sealed connections between the data logger and probe. If this issue was suspected during data collection, the connections were cleaned with compressed air and a deoxidizing spray (De-Oxit) and regreased with a thermally conductive paste. Connection issues were visually obvious since the copper pins in the connectors turn blue when rusted. Several steps were taken to mitigate this re-occurring issue including weather proofing and lifting cable junctions off the ground. However, this pervasive issue continued to some degree throughout the entire study. Similarly, cables would develop kinks resulting in intermittent shorts. Most connectivity issues would manifest when plotted as a noisy signal outside of the typical dT range.

In addition to "noise" we also observed "spikes" most likely caused by power surges. These were usually easy to identify from timeseries plots and often resulted in only a few 15-minute measurements being censored with the data gap then interpolated over. Since the standard deviations of 15-minute minute averages were reported by the data logger it was helpful to sort data by standard deviation to identify high-values often associated with spikes.

Lastly, every plot had at least one power failure during the duration of the study. This was either the result of a tripped GFCI plug that needed to be reset, a power outage from a winter storm, or a malfunctioning trickle charger. Since each TDP station was powered by a 12 V marine-grade deep cycle lead-acid battery that was being charged via 120 V AC outlet, station power remained on for up to 2 days after a power failure. The data produced surrounding a power failure often consisted of many "spikes" that had to be removed. To reduce the amount of effort cleaning data around power failures, a full day of data before and after the power interruption was removed.

Appendix B – Results

Table A-1: Averaged Monthly and Seasonal Transpiration Rates

		1	2	3	4	5	6	7	8	9	10	11	12	Leaf-On	Leaf-Off	Total
	Month:	Jan	Feb	Mar	Apr	May	Jun	Jul	Aug	Sep	Oct	Nov	Dec			
	Average Rainfall (cm):	45.6	18.1	11.8	4.2	6.9	5.9	2.1	1.8	11.0	15.2	17.2	27.9	42.9	124.8	167.6
Douglas-fir	Transpiration (%):	0.2	1.0	4.9	28.6	16.2	15.5	44.6	14.7	3.3	4.0	1.0	0.2	9.8	1.8	3.9
	Rainfall (cm):	0.1	0.2	0.6	1.2	1.1	0.9	1.0	0.3	0.4	0.6	0.2	0.1	4.2	2.3	6.5
Western redcedar	Transpiration (%):	0.1	0.3	1.9	21.8	14.0	12.5	49.4	24.2	1.9	2.1	0.4	0.1	8.6	1.1	0.0
	Rainfall (cm):	0.0	0.0	0.2	0.9	1.0	0.7	1.1	0.4	0.2	0.3	0.1	0.0	3.7	1.3	5.0
Bigleaf Maple	Transpiration (%):	0.2	0.9	1.9	20.0	69.7	72.9	400.6	349.0	28.6	7.9	0.6	0.2	65.8	1.2	0.2
	Rainfall (cm):	0.1	0.2	0.2	0.8	4.8	4.3	8.5	6.2	3.2	1.2	0.1	0.0	28.2	1.5	29.7
Red Alder	Transpiration (%):	0.1	0.8	2.3	16.8	37.3	43.4	223.6	202.3	16.2	3.5	0.5	0.2	36.9	1.1	0.1
	Rainfall (cm):	0.1	0.1	0.3	0.7	2.6	2.5	4.8	3.6	1.8	0.5	0.1	0.0	15.8	1.3	17.1